ISTANBUL TECHNICAL UNIVERSITY ★ EURASIA INSTITUTE OF EARTH SCIENCES

PALEOENVIRONMENTAL CHANGES IN LAKE VAN DURING THE LAST GLACIAL-HOLOCENE

MASTER OF SCIENCE THESIS

Nazik ÖĞRETMEN

Department: Marine and Climate Sciences

Program: Earth System Sciences

June, 2012

ISTANBUL TECHNICAL UNIVERSITY ★ EURASIA INSTITUTE OF EARTH SCIENCES

PALEOENVIRONMENTAL CHANGES IN LAKE VAN DURING THE LAST GLACIAL-HOLOCENE

MASTER OF SCIENCE THESIS

Nazik ÖĞRETMEN
601101011

Department: Marine and Climate Sciences

Program: Earth System Sciences

Thesis Advisor: Prof. Dr. M. Namık ÇAĞATAY

June, 2012

İTÜ, Avrasya Yer Bilimleri Enstitüsü'nün 601101011 numaralı Yüksek Lisans / ~~Doktora~~ Öğrencisi **Nazik ÖĞRETMEN,** ilgili yönetmeliklerin belirlediği gerekli tüm şartları yerine getirdikten sonra hazırladığı **" PALEOENVIRONMENTAL CHANGES IN LAKE VAN DURING THE LAST GLACIAL HOLOCENE"** başlıklı tezini aşağıda imzaları olan jüri önünde başarı ile sunmuştur.

Tez Danışmanı :	**Prof. Dr. M. Namık ÇAĞATAY** İstanbul Teknik Üniversitesi	.....
Jüri Üyeleri :	**Prof. Dr. M. Namık ÇAĞATAY** İstanbul Teknik Üniversitesi	.....
	Prof. Dr. Ömer L. ŞEN İstanbul Teknik Üniversitesi	.....
	Prof. Dr. Naci GÖRÜR İstanbul Teknik Üniversitesi	.....

Teslim Tarihi : **4 Mayıs 2012**
Savunma Tarihi : **4 Haziran 2012**

FOREWORD

I would like to thank to;

My advisor Prof. Dr. M. Namık Çağatay for his continuous support, effort and guideness during my studies and for giving me the opportuinity to be a part of PaleoVan ICDP-Tübitak Project " High resolution water level oscillations of Lake Van during the Late Pleistocene-Holocene" and ITU-EMCOL,

Members of ITU-EMCOL, Emre Damcı, Umut Barış Ülgen, Zeynep Erdem, Demet Biltekin, Dursen Acar and post-member Sena Akçer Ön, for their help, guideness with patience during all my laboratory works,

Collegues from partner institutes of PaleoVan Project,

Prof. Dr. Celal Şengör for his support and encouragement,

My sister Zühre Öğretmen for her limitless patience and support,

My parents Hatice and Ayhan Öğretmen, for their help and support,

My friend Berkay Gümüş for keeping me motivated during my studies, for his endless encouragement and help.

I would like to dedicate this study for my grandfather Mehmet Bedrioğlu and my grandmother Zühre Süleymanoğlu, who passed away.

June, 2012

Nazik ÖĞRETMEN
ITU-EMCOL

TABLE OF CONTENTS

Page

FOREWORD ..... **iii**
TABLE OF CONTENTS ..... **v**
ABBREVIATIONS ..... **vii**
LIST OF TABLES ..... **iii**
LIST OF FIGURES ..... **v**
1.INTRODUCTION **1**
1.1 Scientific Problems, Thesis Objectives and Purpose of the Study 1
1.2 Geology and Limnology and Climatology 3
1.2.1 Geology 3
1.2.2 Limnology 4
1.2.3 Climatology 7
1.3 Previous Work 9
2. MATERIALS AND METHODOLOGY **11**
2.1 Sediment Cores and Sampling Methods 12
2.2 Physical Property Analysis by Multi Sensor Core Logger (MSCL) 12
2.3 Itrax X-Ray Fluorescence (XRF) Core Scanner 16
2.4 Total Organic (TOC) and Total Inorganic Carbon (TIC) Analyses 18
2.5 Stable Isotope Analyses 19
2.6 AMS Radiocarbon (^{14}C) Dating 19
2.7 X-Ray Diffraction (XRD) 20
3. RESULTS **21**
3.1 Lithostratigraphy and Age Model 21
3.1.1 Lithology 21
3.1.2 Age Model 23
3.2 Geochemistry 26
3.2.1 TOC/TIC Values 26
3.2.2 Stable Oxygen and Carbon Isotope Values 26
3.2.3 XRD Results 28
3.2.4 XRF Results 28
4. DISCUSSION **31**
4.1 Abrupt Climate Changes 31
4.2 Lake Level Changes 32
5. CONCLUSIONS **38**
BIBLIOGRAPHY **41**
APPENDICES **45**
RESUME……..**64**

ABBREVIATIONS

AMS : Accelerator Mass Spectrometry
App : Appendix
B/A : Bølling-Allerød
BP : Before present
EMCOL : Eastern Mediterranean Centre for Oceanography and Limnology
Fig : Figure
LGM : Last Glacial Maximum
MIS : Marine Isotope Stage
MSCL : Multi sensor core logger
NAO : North Atlantic Oscillation
NB : Northern Basin
TC : Total carbon
TIC : Total inorganic carbon
TOC : Total organic carbon
XRD : X-Ray diffraction
XRF : X-Ray fluorescence
YD : Younger Dryas

LIST OF TABLES

Page

Table 3.1: AMS 14C dating results, sample ID, composite depth, calibrated age.... 23
Table 3.2: Tephra ages that are used for age model for the last 26 ka in Northerm Basin stratiraphic section (tephra ages after Landmann, 1996, obtained by varve counting)……..23
Table 3.3: Different climate periods during the last 26 ka BP……...24

LIST OF FIGURES

Page

Fig 1. 1: Geology (a), batimetry and drainage area (b) of Lake Van. Geology after Keskin, 2007; Batimetry after Litt et al. (2009)..... 2
Fig 1.2: Schematic diagram showing principal physical, chemical and biological responses of a closed lake system to change in climatic forces (from Battarbee, 2000). 5
Fig 1.3: A. Block diagram showing morphology and structural relations in Eastern Turkey in neotectonical period (from Şaroğlu &Güner, 1981). B.Schematic secitons showing morphology-structure relations and geomorphological evolution of Eastern Turkey (from Şaroğlu&Güner, 1981)..... 4
Fig 1.4: Lake Van region and its position in atmospheric circulation system: Polar Front Jet (PFJ), Subtropical Jet (STJ) and Intertropical Convergence Zone (ITCZ) in winter and summer in the Mediterranean Region, and High Pressure System that influence the climate of the Eastern Mediterranean Region. cP: Continental Polar Air Mass; mP: Marine Polar Air Mass; mT: Marine Tropical Air Mass; cT: Continental Tropical Air Mass (from Litt et al., 2009; after Akçar and Schlüchter, 2005; modified from Wigley and Farmer, 1982)..... 7
Fig 2.1: A schematic configuration of MSCL device ……14
Fig 2.2: Gamma density calibration materials ……...15
Fig 2.4: Front view of the Itrax core-scanner with open hoods……..17
Fig 2.5: Shimadzu TOC/TIC Analyzer …..……19
Fig 2. 6: Bruker D8 Advance XRD device 20
Fig 3.1: Age model based on tephra ages, ^{14}C ages, varv counting and isotopes…...25
Fig 3. 2: Lithostratigraphy and proxy profiles of: TOC/TIC values, $\delta^{18}O$ and $\delta^{13}C$ values of bulk carbonate in Northern Basin stratigraphic section and correlation of $\delta^{18}O$ values of Northern Greenland ice core covering the last 26 ka calBP 27
Fig 3. 3: Graphic of age versus mineral percentages, mineral ratios and stable isotope content of the Northern Basin sediments. 29
Fig 3. 4: XRF results of 26 ka BP 30
Fig 4. 1: Synthetic curve of Lake Van level changes from Kuzucuoğlu et al……36
Fig 4.2: Cross plots and correlation coefficients of different parameters …..……...37

PALEOENVIRONMENTAL CHANGES IN LAKE VAN DURING THE LAST GLACIAL-HOLOCENE

SUMMARY

Lake Van is the fourth largest terminal lake and the largest soda lake in the world (volume 607 km3, area 3,570 km2, and maximum depth 461 m). The pH of its waters is 9.81 and salinity is about 22‰. It is located in the Eastern Anatolian High Plateau in Turkey, with the present lake level located at 1649 m. This region has a continental climate influenced by the Siberian High Pressure, North Atlantic and Mid-Latitude Subtropical systems. Its varved sediments with high sedimentation rate (0.5-0.7 m/ka) provide a continuous record of climatic conditions for Quaternary period.

Multi-proxy analyses, including inorganic XRF Core Scanner elemental, total organic (TOC) and inorganic carbon (TIC), stable carbon and oxygen isotopes of bulk carbonate, and XRD mineralogical analysis, were carried out in the upper part of the 144 m-long composite stratigraphic section recovered by the ICDP-PaleoVan Project in the Northern Basin. The age model was constructed using AMS C-14 analysis and tephra ages from previous studies. The main purpose was to study the paleo-environmental changes during the last glacial-interglacial cycle covering the last 25 ka in the Lake Van region.

The studied composite stratigraphic section consists of five lithological types: a) banded and/or laminated clayey silt, b) homogeneous clayey silt, c) tephra, d) graded sand-silt (turbidite-homogenite), and e) deformed lacustrine sediments and tephra layers (i.e., slide and slump deposits). The time interval between 12.5 and 6.5 ka calBP (Younger Dryas, YD - early Holocene) consists mainly of banded and laminated sediments with tephra intercalations, whereas the interval between 26 and -14.5 ka cal BP sediments are predominantly of graded sand-silt (mass transport deposits) with tephra and homogeneous clayey silt interbeds. The multi-proxy analyses were mainly conducted on the banded and laminated clayey silt and homogeneous clayey silt layers that are authoctonous lake sediments. There is a strong covariance between $\delta^{18}O$ and $\delta^{13}C$ values of the bulk carbonates ($r>0.85$), which demonstrates that the lake remained as a closed basin in general. As a result of geochemical analyses, we obtain very important data regarding to determination of glacial-interglacial periods. After processing all the data, we correlated our study with previous studies.

SON BUZUL-HOLOSEN DÖNEMLERİ SÜRESİNCE VAN GÖLÜ'NÜN PALEOÇEVRESEL DEĞİŞİMLERİ

ÖZET

Van Gölü 607 km3 hacme ve 3,570 km2 alana sahip dünyanın en büyük 4. kapalı gölü ve en büyük soda gölüdür. Doğu Anadolu Yüksek Platosu'nda yer alan bu göl, coğrafik konumu nedeniyle Sibirya Yüksek Basınç, Kuzey Atlantik ve Orta-Enlem Tropik iklim sistemlerinin etkisinde kalmaktadır. Aynı zamanda denizden de oldukça yüksek olması (1648 m), kurak bir iklime sahip olmasına sebep olmaktadır. Hem konumu hem de kapalı bir havza oluşu, varvlı bir çökel yapısı ile Kuvaterner (GÖ 2.5 My) süresince önemli bir paleoiklimsel kayıt oluşturmasına olanak vermiştir. Bu nedenle Kuvaterner dönemi içinde yer alan Son Buzul (26,000 GÖ) ve Holosen (11,500 GÖ) dönemleri süresince meydana gelen iklimsel değişimleri (yağış, buharlaşma, göl seviyesi değişimleri) araştırmak amacıyla bu gölden 2010 yılında Uluslar arası Kıtasal Sondaj Programı kapsamında alınan çökel karotlarında çeşitli fiziksel ve kimyasal analizler yapılmıştır. Bu analizlerden Çok Sensörlü Karot Loglayıcısı (MSCL) ile göl çökellerinin fiziksel özelliklerinin incelenmesi, X-Ray Fluorescence (XRF) ile elemental özelliklerin araştırılması, TOC/TIC Analizörü ile organik-inorganik karbon içeriğinin saptanması çalışmaları İTÜ-EMCOL laboratuarlarında; X-Ray Diffraction ile mineralojik özelliklerin incelenmesi çalışması İTÜ-jeoloji Mühendisliği Departmanı, X-Işınları Laboratuarı'nda yapılmıştır. C-14 yaşlandırmaları ve duraylı izotop analizleri için seçilen örnekler yurtdışındaki laboratuarlara gönderilmiştir.

Van gölü sediman karotlarında temel olarak 5 ana birim tayin edilmiştir. Bunlar: a) bantlı/laminalı killi silt, b) homojen killi silt, c) tefra, d) dereceli kum-silt (türbidit-homojenit) ve e) deforme göl sedimanı ve tefra tabakaları. GÖ 12.5-6.5 ky arasındaki dönem (Younger Dryas-erken Holosen) genel olarak tefra ara katmanlı bantlı-laminalı sedimanlar ile temsil olunurken GÖ 26-14.5 ky arasındaki dönem tefra ara katmanlı dereceli kum-silt ile temsil olunur. Jeokimyasal analizler çoğunlukla gölün kendi çökelleri olan bantlı ve laminalı sedimanlar ile homojen çamurdan alınan örneklerden yapılmıştır. Analizler sonucunda $\delta^{18}O$ ile $\delta^{13}C$ arasında gölün kapalı bir havza olarak kaldığına işaret eden güçlü pozitif bir kovaryans ($r>0.85$) olduğu gördük. Bu analizler, buzul-buzul arası dönemleri tayin etmemiz açısından önemli veriler sunmuştur. Verilerin üzerinde yaptığımız çalışmaların ardından, daha önceki çalışmalar ile karşılaştırma yaptık.

1.INTRODUCTION

Investigating the causes of climate change during the Quaternary (last 2.588 Ma) is significant considering the impact of the climate changes on environment and human life. Paleolimnological studies are useful to obtain the past climate records using organic and inorganic proxies, which provide information on evaporation/precipitation ratio, temperature, chemical and biological changes in the water column. In general, lakes display higher organic productivity and sedimentation rates than oceans and allow high resolution regional paleoclimatic and paleoenvironmental analyses.

Lake Van, which is "Van Gölü" in Turkish, is located in the Eastern Anatolian High Plateau in eastern Turkey, with the present lake level located at 1649 m, lying at about 43°E longitude and 38.5°N latitude. This region has a continental climate influenced by the Siberian High Pressure, North Atlantic and Mid-Latitude Subtropical systems (Akçar and Schlühter, 2005). The pH of its waters is 9.81 and salinity is about ‰ 22. Its varved sediments with high sedimentation rate (0.5-0.7 m/ka) provide a continuous record of climatic conditions for Quaternary period (Kempe *et. al.*, 1978.).

This thesis was carried out in the context of International Continental Drilling Program (ICDP) PaleoVan Project and funded by TUBITAK project "Water Level Oscillations of Lake Van during the late Pleistocene-Holocene" and carried out at İTÜ-EMCOL. For the purpose of studying the sedimentary records of climate and lake level changes, multi-proxy analyses were performed in the upper 50 m of the 144 m-long composite stratigraphic section recovered by the ICDP (International Continental Drilling Program)-Paleo Van Project in the Northern Basin. These multi-proxy analyses consist of inorganic XRF (X-Ray Fluorescence) Core Scanner elemental, TOC (total inorganic carbon) and TIC (total inorganic carbon), stable oxygen ($\delta^{18}O$) and carbon ($\delta^{13}C$) isotopes of bulk carbonate, XRD (X-Ray Diffraction) mineralogical analysis, MSCL (Multi Sensor Core Logger) physical properties and AMS ^{14}C dating analysis.

1.1 Scientific Problems, Thesis Objectives and Purpose of the Study

The following scientific questions regarding the Lake Van can be asked:

1. What are main factors causing lake level variation during the Last Glacial-Holocene?

2. How Lake Van sedimentary record compare with similar records in the region elsewhere?

3. Which proxies can be used to determine lake level variations?

The objectives of this thesis are to answer the above questions using sedimentological, geochemical and physical analysis of core sediments recovered at a water depth of 245 m from the western part the lake (Northern Basin, Fig. 1.3). Drilling operation within the framework of the International Continental Drilling Project "Paleo Van", was performed by an DOSECC (Drilling, Observation and Sampling of the Earths Continental Crust) during July-August 2010. Northern Basin was selected on the basis of its high sedimentation rate and proximity to Quaternary volcanics. In total 140 m long core collected from different 4 core holes in Northern Basin (NB) (Fig.1.1).

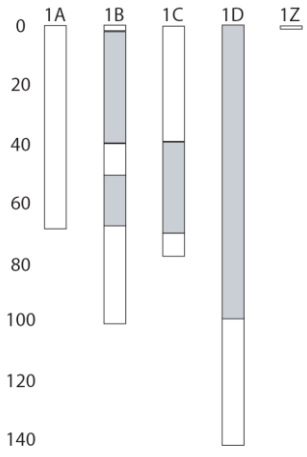

Fig 1. 1: Northern Basin drilling site holes (white columns represent recovered cores)

In order to examine influences of paleoclimatic changes, the results have been compared with similar regions such as Lake Zeribar (Iran) and Lake Frassino (Italy).

Because of characteristic structure and stability of Lake Van as an endorheic basin (Fig. 1.2), this study includes important results which probably lead future world-wide detailed investigations.

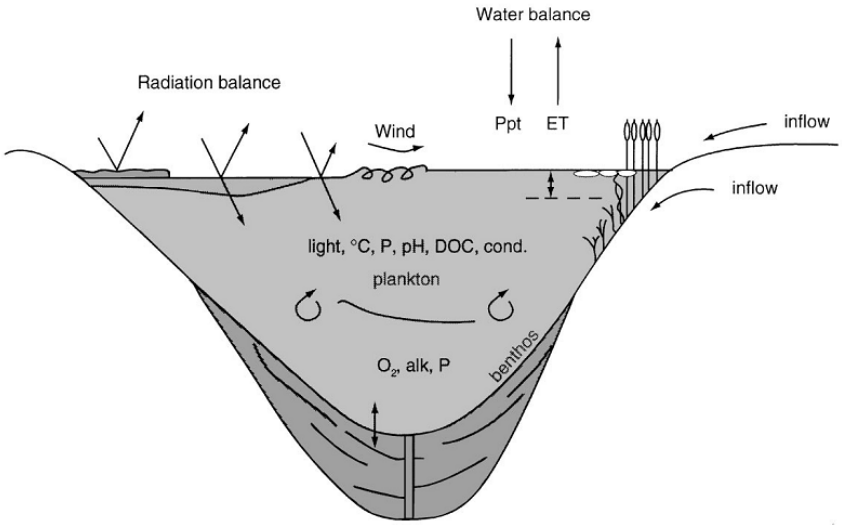

Fig 1. 2: Schematic diagram showing principal physical, chemical and biological responses of a closed lake system to change in climatic forces (from Battarbee, 2000). Ppt: precipitation, ET: Evapotranspiration, P: phosphorus, DOC: dissolved organic carbon

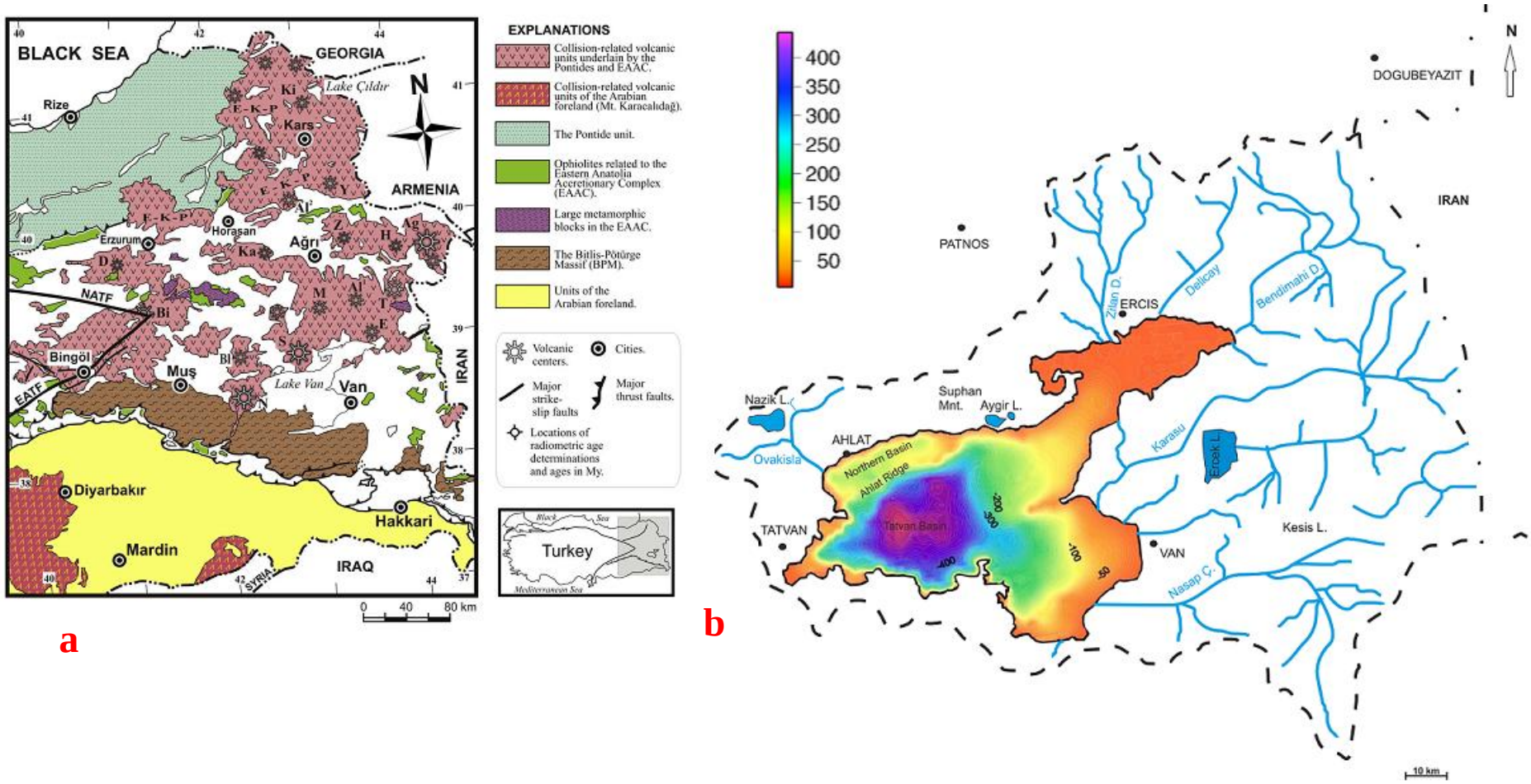

Fig 1. 3: Geology (a), batimetry and drainage area (b) of Lake Van. Geology after Keskin, 2007; Batimetry after Litt et al. (2009)

1.2 Geology and Limnology and Climatology

1.2.1 Geology

Subsidence of the Muş-Van Basin has originated through a combination of normal and strike-slip faulting and thrusting (Sengör et al., 2008). This subsidence was triggered by the gradual collapse of the magma chamber that fed the Nemrut Volcano, which is one of a series of volcanoes in the region, related to the regional tectonics associated with the closure of Tethys (**Degens** et al., 1984).

Neotectonic evolution of Eastern Anatolia has started with the existence of peneplain geomorphology in Middle Miocene (15.97 -11.608 Ma BP). In the beginning of neotectonic evolution of Eastern Anatolia, sediments have deposited in the shallow and large lakes or in river environments synchronously. Due to tectonic forces, east-west trending inclined folds have generated and the region has become undulated. However, accelerated rate of folding exceeding the erosion resulted in generation of undulated topography. The elevation between ridges and basins increased as the drainage basin was forming (Fig.1.4).

Not only the tectonic activity but also accompanied volcanism has caused variations on morphology such as asymmetry of folds, east-west trending vertical/close to vertical thrusts developed at the north-south borders of the basins such as the elongated Muş Basin (Şaroğlu and Güner, 1981; Dewey et al., 1986; Şengör et al., 2008). N-S trending tensional fissures that intersect with each other have developed parallel to the direction of compression facilitating suitable environment for possible volcanic eruptions. During the compressive phase, the calc-alkalic magmas extruded through Süphan and Ararat Volcanoes, whereas extensional phase in the region is characterized by alkalic volcanism in Tendürek and Nemrut Volcanoes.

Lake Van-Muş Basin was separated into two sub-basins as consequence of eruption of Nemrut Volcano from vertical transacting tensional fissures, forming the Lake Van basin to the east (Şaroğlu and Güner,1981).

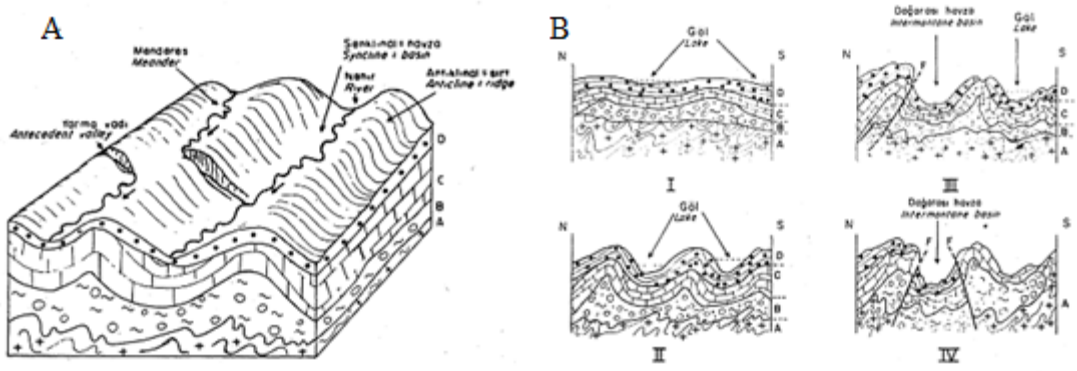

Fig 1.4: A. Block diagram showing morphology and structural relations in Eastern Turkey in neotectonical period (from Şaroğlu &Güner, 1981). B.Schematic secitons showing morphology-structure relations and geomorphological evolution of Eastern Turkey (from Şaroğlu&Güner, 1981)

1.2.2 Limnology

Lake Van is the fourth largest terminal lake and the largest soda lake in the world (volume 607 km^3, area 3,570 km^2, and maximum depth 461 m). It is bordered by the Nemrut Vaolcano to the west, Süphan Volcano to the north, Bitlis metamorphic massif to the south, and Eastern Anatolian Accretionary Complex (EAAC) to the east (Fig. 1.3a).

It has 12.470 km^2 drainage basin fed by mostly Bendimahi and Zilan rivers carrying fresh water to the lake (Fig. 1.3b). Total water loss of Lake Van by evaporation is annually 4.2 km^3 /yr and total water inflow by precipitation is 2.5 km^3/yr and by rivers 1.7 km^3/yr (Reimer et al., 2009).

During winters, the temperature in the region is generally below 0°C. The temperature of lake water at the surface is around 20-23°C during summer, and around/below 0°C during winters (Kempe, 1978). Waters of Lake Van have a stratified structure; in summers, dilution of the warmer water layer (epilimnion) with fresh water carried by the rivers, results in forming a stable surface layer. Because of the seasonality, during cold seasons, epilimnion gets colder and denser, and cold water sinks to the hypolimnion. This mixing through the year, enables the lake water stay oxygenated where the mixing occurs. Thermocline development is observed in the late spring and summer. Gradational increase of air temperature results in

migration of isotherms within the water column and pycnocline moves to the depth of 50 m at the end of summer. Decreasing temperature in autumn and winter leads to

destruction of thermocline; therefore hypolimnion loses its stability at the temperature of maximum density. This transfer between water layers because of density instability results in overturn of the entire lake in a few months and oxygen is carried through greater depths (Degens et al., 1984). However, during periods of high river water inflow and high water levels, renewal (ventilation) of the deep waters in the lake is prevented by the water stratification, causing anoxic conditions below depths of -300 m (Kipfer et al., 1994).

The varve structure of the Lake Van sediments form as a result of seasonal sedimentation producing a three-laminae structure in a year (Kempe et al., 2002; Stockhecke et al., 2012)Sediment trap studies, together with detailed geochemical and scanning electron microscopy analysis of cores, show that an annual varve consist: 1) a non-skeletal algal and detrital mineral-rich lamina deposited during spring, 2) a light carbonate-rich lamina formed during the summer by evaporation, and 3) siliceous frustules-rich laminae formed during autumn and winter (Stockhecke et al., 2012).

Litt et al. (2009) indicated that, due to the high alkalinity, silica containing organisms are not preserved after the cell death. Our studies indicate that the ostracoda shells exists in the lake sediments, but arere mostly juvenile and too weak to separate from the bulk sediment. *Limnocythere inopinata* is the most common species in Lake Van, followed by *Candona* sp. and *Cyprideis* sp. genera. Except for the ostracoda shells, there are no macrofossils in the sediment cores.

Short term lake level changes of a few meter occur in the lake that have been related to the activity of the sun spots having periodicity of 10-11 years (Kempe, 1978) (Fig. 1.5). High solar activity causes weather conditions to become more unstable with increased amount of rainfall, decreased evaporation and higher humidity, and results in lake level rise (Degens et al.,1984)

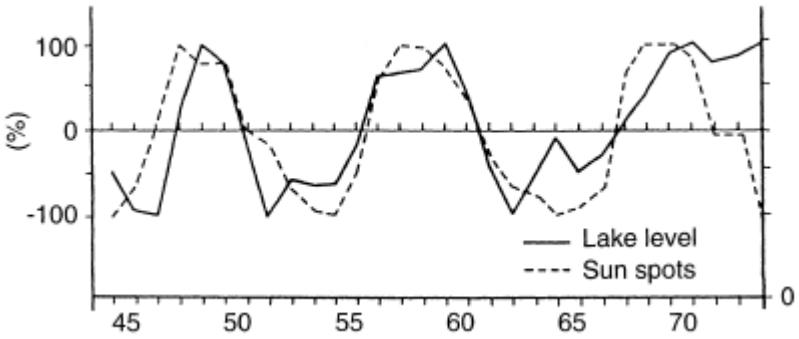

Fig 1.5: Relation between lake level and the quantity of sun spots between 1944-1973 from (Kempe, 1978)

Lake Van is a saline lake which has an alkalinity of 155 mmol/l and pH of 9.80, in the Northern Basin (NB) pH is around 9.07, and its salinity is about ‰ 22 (Reimer et al., 2009). The dominant anion in the lake water is bicarbonate ($HCO3^{-}$) and dominant cation is sodium (Na^{+}) that balances bicarbonate concentration. This situation explains the reason of development of Lake Van as a soda lake (**Degens** et al.,1984).

1.2.3 Climatology

Lake Van region is has continental climate properties showing high humidity, having low temperature around the lake directly related to geographic location. This region has a continental climate influenced by the Siberian High Pressure, North Atlantic and Mid-Latitude Subtropical systems that determine the boundary between humid Mediterranean and continental climate (Fig. 1.5) (Akçar and Schlühter, 2005; Litt et al., 2009; Wick et al., 2003). Ascendant southwesterly subtropical winds from eastern Mediterranean cause precipitation during autumn, winter and spring, whereas dry summers are related to continental air masses (Wick et al., 2003).

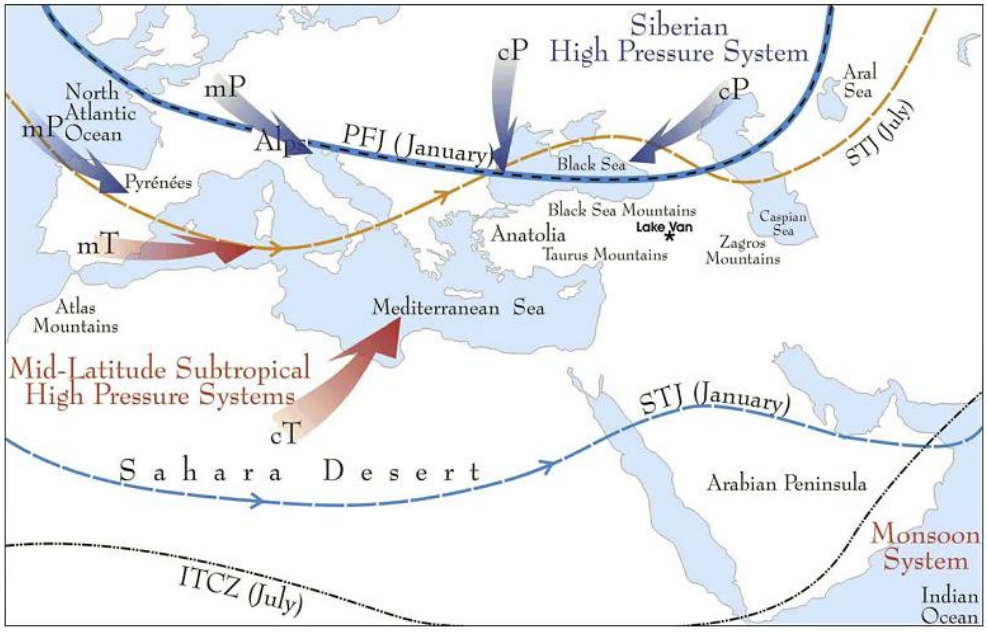

Fig 1.5: Lake Van region and its position in atmospheric circulation system: Polar Front Jet (PFJ), Subtropical Jet (STJ) and Intertropical Convergence Zone (ITCZ) in winter and summer in the Mediterranean Region, and High Pressure System that influence the climate of the Eastern Mediterranean Region. cP: Continental Polar Air Mass; mP: Marine Polar Air Mass; mT: Marine Tropical Air Mass; cT: Continental Tropical Air Mass (from Litt et al., 2009; after Akçar and Schlüchter, 2005; modified from Wigley and Farmer, 1982).

Siberian High Pressure (Siberian Anticyclone): Siberian High Pressure (SHP) forms at the latitudes between 20-40 degrees from the equator, as a result of uplifting air at the equator. Raising hot air cools, loses its moisture, and it is transported poleward where it sinks, creates a high pressure area. SHP is generally centered around Lake Baikal bringing a massive collection of cold and cold dry air that accumulates on Eurasian terrain. Siberian High is the

strongest semi permanent high in northern hemisphere and responsible for both the lowest temperature (-67.8°C) and the highest pressure (1083.8 mbar) that ever occurred. In general temperature is lower than -40°C, and the sea level pressure is above 1040 mbar (D'Arrigo et al., 2005).

North Atlantic Oscillation (NAO): NAO stands for the pressure differences between Azores (30°N) and Iceland (60°N). It carries wet and warm or dry and cold air in winters to northern Europe. NAO occurs in two phases. Positive NAO in winters occurs when there is a large pressure difference between Azores and Iceland and results in generation of more and stronger storms crossing the Atlantic travelling in a northeasterly direction. These air movements bring heat from the ocean to northwestern Europe leading warm and wet winters in Europe but cold and dry winters in Mediterranean. Negative NAO winters occur when there is a small pressure difference between Azores and Iceland. As a result, less and weaker storms are generated. Such storms mostly follow more southerly track than positive NAO and bring warm and wet air to Mediterranean and cold and dry air to northern Europe (Visbeck et al., 2001).

Mid-Latitude Subtropical High Pressure: Generally carries warm and humid air mass with mild winters. It extends from 30 to 60 degrees of latitude mainly on the eastern and western borders of continents. This westerly wind blows from high pressure area towards poles from west to east steering the extra-tropical cyclones. It is strongest in the winter and weakest in the summer. The Westerlies are significant in carrying warm, equatorial waters and winds to western coasts of continents. Mid latitude subtropical high pressure systems bring continental and marine tropic air masses towards Turkey.

In the Lake Van region, precipitation mainly occurs as snowfall in winters and as rainfall in the late springs. During the other seasons, volume of precipitation is quite low therefore temperature and evaporation values are measured in small quantities. Monthly temperature averages during winter are below 0°C from December to February and around 20°C during the summer. Annual temperature difference is mostly more than 25°C which is unique for the whole (Erinç, 1953). 27% of precipitation in Lake Van region is supplied during winter seasons. The mean annual precipitation of the lake amounts to 300-400 mm along the north and east side, whereas 600-800 mm fall to the south of the lake up to 1000 mm in the southwestern

mountains related to snowfall. The snow melt in the mountains that occurs in late April to June causes remarkable lake level fluctuations because of river runoff up to 90 cm seasonally (Landmann et al., 1996). Due to seasonal precipitation and evaporation, the lake level increases from January to June and decreases from June to January, with an amplitude of 40-50 cm (Kadioglu et al., 1997).

1.3 Previous Work

In Lake Van region, several studies carried out starting with Parrot (1834), Abich (1856) and Sieger (1888) about the soda chemistry of the lake water, eruptions or just personal observations during trips. Detailed modern investigations started in 1970s mainly by German and Swiss researchers such as Degens, Kempe and Kazmierczak.

Parrot (1834); wrote a book of his own experience about his travel to Mount Ararat (Ağrı Dağı) in order to make a research about Noah's ark. As a naturalist, he wrote his observations and published a book including geological properties, magnetic observations, temperature and barometrical measurements of the regions that he travelled through the Caspian Sea and the Black Sea. According to his barometric measurements, the editor of the English version of the book, attached the appendixes part and summarized the scientific papers of Parrot's about shoreline differences between the Black and Caspian Seas.

Abich (1856); made observation surroundings of Mount Ararat and examined tectonic structure of the region indicating the formation of conical volcanoes in the region and the preceeding deep dynamic disturbances at the end of Tertiary time.

Sieger (1888); studied lake level fluctuations of East Anatolian lakes (Reimer et al., 2009; Sieger, 1888).

Erinç (1953); investigated in detail the general geography of Eastern Anatolia. This study included climatology, human geography, morphology and vegetation. In addition, he also reported level changes of Lake Van covering the last few centuries combining the studies of previous works and his own observations.

Kempe, Degens and Kurtman (1978) made an expedition to Lake Van and published the preliminary results in an international publication and in the MTA Volume. This expedition included sediment coring, seismic operations and hydrochemistry sampling. As a result of these studies, they indicated that the Holocene lake level fluctuations are correlatable with solar activity.

Degens *et al.* (1984); studies about geology, hydrochemistry, tectonics and sediment structure studies were carried out and they examined the study field as three physiographic provinces: lacustrine shelf, sub-lacustrine shelf and lake basin. Using sediment cores, they prepared a lake-wide stratigraphic correlation with the help of barker beds such as ash layers and micro-laminations.

Kipfer *et al.* (1994); analyzed deep water renewal of Lake Van as vertical mixing, measuring helium, tritium and neon concentrations and relations to mantle injection into the lake.

Landmann *et al.*(1996); performed significant exploring surfacing climatic lake level changes of the region studying on varved structures of Lake Van sediment cores.

Kadıoğlu, Şen and Batur (1997); used the recent lake level measurements and claimed that changes in lake level was controlled by sun spots and meteorological variability.

Akçar and Schlühter (2005); made a research based on paleoglaciation of Anatolia and linked to recent climate changes of the region considering the main atmospheric systems that influenced Anatolia.

Keskin (2007); made an advanced volcanological study of Eastern Anatolia and studied the magma types of the volcanic units.

Şengör *et al.* (2008); performed a detailed study about tectonic evolution of Eastern Turkish high plateau as a Turkic-type orogeny and its relation to magmatism.

Litt *et al.* (2009); published the results of studies sediment cores, involving palynological and oxygen isotope analysis, extending the climate record to the Last Glacial Maximum (LGM). This study also presented seismic profiles that was used for the planning of the ICDP- PaleoVan Project, having the objectives of studying long records of climate, dynamics of lake level fluctuations, and volcanic and seismic activities.

Reimer, Landmann and Kempe (2009); published a paper which is focused on hydrochemistry and the history of Lake Van. This study is one of the key studies which emphasizes geochemical approaches on lake sediments (mineralization, salt content, organic productivity) and chemical structure of water column (salinity,pH

showing differences in evaporation, precipitation and temperature over the last several thousand years.

Huguet *et al.* (2011); reported a detailed organic chemistry study carried out in order to investigate organic productivity, seasonality and stratification of Lake Van using biomarkers as tools. In addition, they evaluated the potential use of paleotemperature proxies derived from the long chain alkenones and glycerol dialkyl glycerol tetraethers.

2. MATERIALS AND METHODOLOGY

This chapter describes the lithological properties of the sediment cores and analytical methods used to analyze the cores. In the framework of the ICDP PaleoVan Project, four holes were drilled to a depth of 144 m below lake floor (mblf) in the Northern Basin of Lake Van. Over 100 drill core sections with a diameter of 7 cm were collected from Northern Basin.

2.1 Sediment Cores and Sampling Methods

Sediment cores from the Northern Basin of Lake Van were drilled during 1stJuly-26th August 2010. The cores were analyzed for physical properties by Multi Sensor Core Logger (MSCL) and transported to to IODP Core Repository at the University of Bremen. In January 2011, lithological description and sampling of the cores were carried out by ITU EMCOL scientists and a composite stratigraphic section was generated for the Northern Basin drill site. 10 cc discrete samples at 10 cm interval of laminated and banded sediments were collected from the master section of the cores, with most of the mass flow and tephra layers being excluded from sampling. The descrete samples were used for total organic (TOC) and total inorganic carbon (TIC) analysis, stable isotope analyses of bulk carbonate and XRD mineralogical analyses. Some microfossil studies (Ostracoda) from laminated levels were also made. U-channel samples of NB sediment cores were also collected for XRF Core Scanner analysis at the İTÜ-EMCOL Core Analysis Laboratory.

2.2 Physical Property Analysis by Multi Sensor Core Logger (MSCL)

MSCL analyses carried out in the field camp in Ahlat using İTÜ EMCOL Geotek Multi Sensor Core Logger. This device is set up for measuring high resolution physical properties of sediment cores such as magnetic susceptibility, gamma density, electrical resistivity and P-wave velocity (Fig. 2.1).

Each sensor measures specific physical property of the core as the core is pushed in steps, controlled by the laser caliper, to pass through the sensors. The analytical

results are saved automatically under the control of a special software program based on "Windows" operating system. MSCL equipment is capable to measure sediment cores up to 150 cm long and 5 to 15 cm diameter with a resolution of up to 0.5 cm. In addition, scanning continues without disturbing the sample even if the cores are not whole but split ones (GeoTek, 2012).

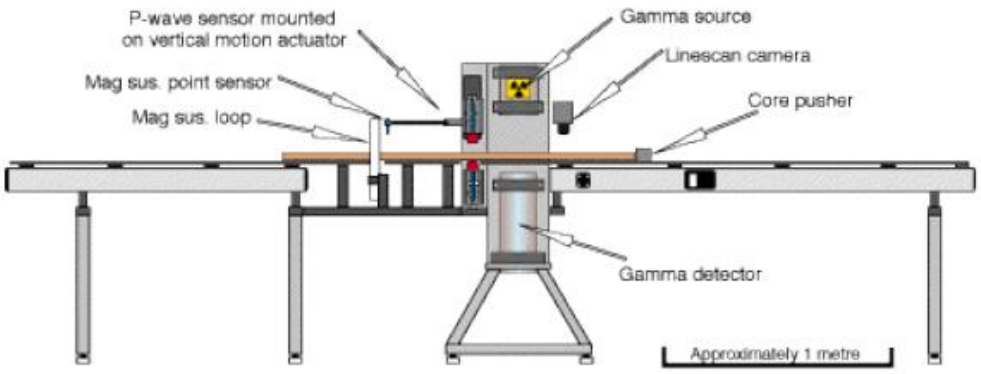

Fig 2.1: A schematic configuration of MSCL device

The main measurements of Geotek MSCL device are abbreviated below (webpage of Geotek MSCL, 2012):

Temperature: In order to provide stable conditions during measurement, temperature of the room and the cores are supposed to be measured 0.01 °C sensitivity by a PRT (platinum resistance thermometer) probe.

Gamma Density: Gamma density is measured by 2 components which are gamma ray source and detector affixed to the device. Via measuring gamma density, porosity, mineral and grain density can be calculated obtaining high resolution data. These analyses are performed by a beam of emitted gamma rays (photons) from Cs-137 source and meeting the detector passing through the core. The number of transmitted photons demonstrates the density of the sediment core and helps to determine the material. Calibration of the measurement is processed by a cylindrical aluminum material with pieces of different diameter which are surrounded by distillated water representing the sediment thickness (Fig. 2.2).

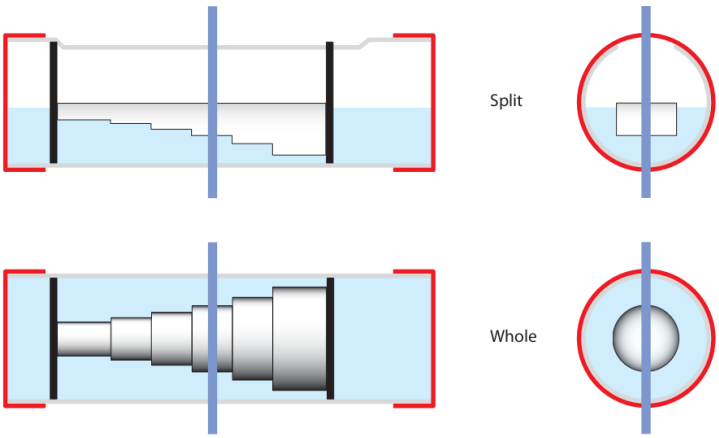

Fig 2.2: Gamma density calibration materials

P-wave velocity: This measurement aims to determine physical features of the sediment cores by Acoustic Rolling Contact (ARC) transducers (Fig.2.3). The role of the transducers is providing suppressed data of physical properties of the cores which are purified from internal ringing and back radiation. This process is performed by an active element of transducers which combines high coupling with relatively low acoustic impedance. Transducers are to achieve precise, high quality and repeatable results, which are obtained by the high S/N (signal to noise) ratio resulting from the use of the lower frequency and good coupling combined with the bandwidth, from cores of almost any composition in diameters from 50 to 150 mm.

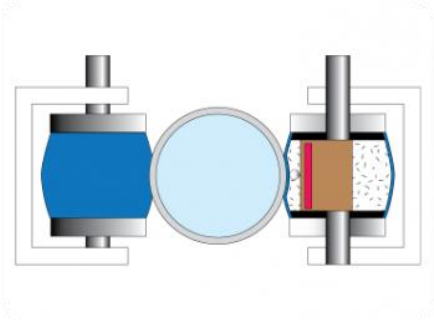

Fig 2.3: Cross section of rolling transducers

Non-Contact Electric Resistivity (NCR): The NCR technique operates by inducing a high frequency magnetic field in the core, from a transmitter coil, which in turn induces electrical currents in the core which are inversely proportional to the resistivity. Very small magnetic fields regenerated by the electrical current are measured by a receiver coil. This technique

provides the requisite accuracy and stability required. Resistivities between 0.1 and 10 ohm-meters can be measured at spatial resolutions along the core of approximately 2cm.

Calibration is achieved by filling the core liner with water of known salinities (and hence known resistivities).

Magnetic Susceptibility (MS): MS is the degree of magnetization of a material in response to an applied magnetic field**.** Positive MS values point out the materials such as ferromagnetic, paramagnetic etc. inferring strengthen magnetic field by the presence of such materials; however, negative MS values which are weakened show diamagnetic material presence. Changes in MS correlate with changes in sedimentary provenance and/or diagenetic environment. MS records are frequently used for inter-core correlation. For whole core sections Bartington loop sensor (MS2C) and for split cores Bartington point sensor (MS2E) can be used. Calibration for this measurement is done by measuring a single standard sample of a stable iron oxide which has been tested and analyzed by the manufacturer (Bartington). The magnetic susceptibility sensor is electronically set to measure this standard sample.

2.3 Itrax X-Ray Fluorescence (XRF) Core Scanner

Itrax Core Scanner is one of the latest developments in non-destructive analytical instrumentation aimed at paleoclimatic research (Fig.2.4). This equipment is set up in İTÜ-EMCOL Core Analysis Laboratory.

Itrax Core Scanner provides high resolution optical and radiographic images and elemental profiles of sediment cores and sediment u-channels with a diameter between 2-12 cm and length up to 180 cm. This instrument consist of a central measuring tower incorporating an X-Ray focusing unit and a range of sensors which are optical-line camera, laser topographic scanner, X-Ray line camera for measuring the transmitted X-Rays and high count rate XRF detection system. It is optional to scan entire length of samples or cores from centimeter to 200 µm.

Northern Basin u-channels were analyzed during this study with 500µm step-size, counting for 10 seconds, and optical image resolution is 50µm pixel^{-1} for sediment cores in order to analyze intensity of following elements: Al, Si, P, S, Cl, Ar, K, Ca,

Sc, Ti, V, Cr, Mn, Fe, Co, Ni, Cu, Zn, Ga, Ge, As, Se, Br, Rb, Sr, Y, Zr, Nb, Mo, Cd, Sb, I, Cs, Ba, La, Ce, Hf, Ta, Pb, Th, U.

Fig 2.3: Front view of the Itrax core-scanner with open hoods

Instrumental component and XRF detection systems are summarized briefly below:

Optical camera system is used to generate good quality RGB digital images of the sample surface before the X-Ray scan begins with a maximum resolution of 50µm $pixel^{-1}$.

Digital X-Ray line camera is used for recording the intensity of X-radiation transmitted through the sample; low density areas appear in light color and higher density areas appear in dark color.

X-Ray source and focusing is provided using 3kW X-ray generator and can be used with different tube anodes to obtain excitation for a range of elements. The current system uses a 3kW Mo target tube that can operate up to 60 kV and 50 mA, but the actual voltage-current selected can be optimized for the elements required. Analyses were performed selecting 50 mA current and 45 kV voltage settings.

The XRF detection system: To obtain reliable data sample-detector distance is kept constant and the Itrax achieves this by using a laser triangulation system to measure the topography of the sample surface. Detection is processed vertically adjusting the detector itself according to the topographic scan data previously acquired.

The Itrax scanner is controlled from a central computer that runs on a Windows XP platform. Through a graphical user interface called Core Scanner Navigator where standard operation

procedures can be implemented and monitored, system can be controlled. Q-Spec is the second program which provides interaction with the interface and compensates for a refined XRF fundamental parameters model for inter-element effects and to enable the conversion of count rates to concentration.

2.4 Total Organic (TOC) and Total Inorganic Carbon (TIC) Analyses

TOC / TIC analyses were carried out in İTÜ-EMCOL Sedimentology and Geochemistry Laboratory using Shimadzu TOC/TIC Analyzer from core sediment samples (Fig.2.5). Samples of mostly laminated intervals and some from homogenous mud levels of the cores were dried using freeze dryer technique. Dried samples are pounded into finest size to homogenize before the analysis. Approximately 50 mg from each sample section was used for the analysis.

Before beginning analyses, calibration for TC and TIC is applied in order to use further analyses, for the calibration of total carbon analysis, potassium hydrogen ftalat [C_6H_4 ($COOK$)($COOH$)] with 204.22 molecule weight and 47.05 weight percentage; for total inorganic carbon sodium hydrogen carbonate ($NaHCO_3$) with 1200 molecule weight and 14.28 weight percentage is used. By combusting 10, 20 and 40 mg potassium hydrogen ftalat, calibration curves are created for total carbon and similar process is applied for creating inorganic carbon curves burning sodium hydrogen carbonate in 20, 40 and 80 mg. Total carbon (TC) percentage is calculated after combustion of the sample at 900°C. TIC percentage is estimated adding using 85% phosphoric acid to the sample and heating the sample at 200°C and then measuring the amount of CO_2 evolved. Combustion and acid treatment processes for both TC and TIC are performed in solid sample module using pure oxygen. TOC percentage is calculated from the following formula: $TOC = TC - TIC$. All the steps during the tests are controlled from a specific software program that is built for this analyzer. These analyses have the precision of 1% at 95 % confidence level.

Fig 2.4: Shimadzu TOC/TIC Analyzer

2.5 Stable Isotope Analyses

Weakness of the shells and minority of the ostracoda from the same species prevented stable oxygen and carbon isotope analyses from the ostracod shells. However, $\delta^{18}O$ and $\delta^{13}C$ analyses were performed from the bulk carbonate of mostly the laminated sediment samples, representing the autochthonous sediments of the lake. Samples are pounded into finest size before sending for analyses to University of Arizona, Environmental Geochemistry Laboratory, U.S.Ai by mass spectrometry. This measurement runs with a single ion detector and allows isotope ratio measurements with precisions between ~0.02% and 1% for the the stable isotope measuements (Becker, 2002).

2.6 AMS Radiocarbon (^{14}C) Dating

Accelerator Mass Spectrometry (AMS) method was used for determining the ages of plantmaterial in Lake Van samples. A total of three samples with weight of >1 mg have been sent to University of Arizona, Environmental Geochemistry Laboratory, U.S.A. for analyses (Table 1). Samples are taken from laminated levels after washing them in distilled water using a 63µm sieve. After sieving, the remaining plant materials are dried and examined under a microscope. The collected plant fragments are inserted in 10% dilute hydrochloric acid (HCl) in order to winnow out the carbonaceous clayey materials and washed under distilled water 3-4 times. The paln material is then dried at temperature of 50°C, before sending for AMS ^{14}C analysis. The ^{14}C ages were converted to calendar year using IntCal option of Calib V6.1 programme (Reimer et al., 2004).

2.7 X-Ray Diffraction (XRD)

XRD analyses of the powder samples are were analyzed using Bruker D8 Advance X-Ray diffractometer located in X-Ray Laboratory of Geological Engineering Department in ITU (Fig.2.6). Samples are pounded using agate mortar to finest size and put in special sample dishes. The auto sampler of device is capable of storing 9 samples, each analysis taking approximately 16 minutes. The device measures the distance between atomic layers (*d*-spacing), intensity (*I*) of mineral in bulk material and reflection angle (2Θ- 2 theta) from mineral atomic surfaces of inorganic and crystalline materials.

Fig 2. 5: Bruker D8 Advance XRD device

Measurement is controlled from a central computer software program on Windows operator system and through a graphical interface. Diffractograms are obtained showing peaks of minerals and *d-spacing*, 2Θ values and peaks of requested minerals. In addition to the software that device is connected, it is possible to process the raw data using a different software program called MacDiff 4.1.2 on Apple Macintosh operator system which is freeware and non-profit created by Dr. Rainer Petschick (Petschick, 2000). In order to obtain the diffractograms on MacDiff 4.1.2, there is a need to convert the raw data (.raw format) into compatible .RAW format using File Buddy converter program (Bisson, 2012).

3. RESULTS

3.1 Lithostratigraphy and Age Model

3.1.1 Lithology

The description of related sediment cores and their lithological properties are summarized in this section. In total, 48 core sections were described from four different holes arranged according to a composite depth in a master section for the Northern Basin site. The total 50 m length of the cores cover the last 26,000 years, according to the established age model based our three ^{14}C analysis, tephra ages of Landmann et al. (1996b) and Sumita and Schmincke, (2011), and varve-counting (see below).

The studied composite stratigraphic includes five lithological types: a) banded and/or laminated clayey silt, b) homogeneous clayey silt, c) tephra, d) graded sand-silt (turbidite-homogenite), and e) deformed lacustrine sediments and tephra layers (i.e., slide and slump deposits).

a) *Laminated and/or banded clayey silt:* These sediments are mainly composed of red, green, brown and occasionally green and grey colored laminated and banded muds. The laminae have thickness of less than a mm and bands range up to several cm in thickness. The laminae consists of mainly carbonate and detrital mineral and organic matter components, and are seasonally deposited. In Northern Basin (NB) site, the laminated and banded sediments form only 20.1% diment cores of the composite section.
b) *Homogenous clayey silt:* This litho-type is light gray to light brown homogeneous clayey silt mud, showing no size gradation. It is interbedded with laminated and banded muds, being part of normal autochtonous lacustrine sediments. They commonly have lower TIC contents than the laminated and banded muds.
c) *Tephra layers:* The tephra layers have sand size and mostly air fall deposits. They occasionally contain lapilli having a diameter of 2-3cm. Tephra layers have thickness ranging from few mm to several cm, and in color from black, brown to dark grey. They have mostly alkaline affinity from Nemrut Volcano, with minor tephra of calc-alkaline composition originating from Süphan Volcano.

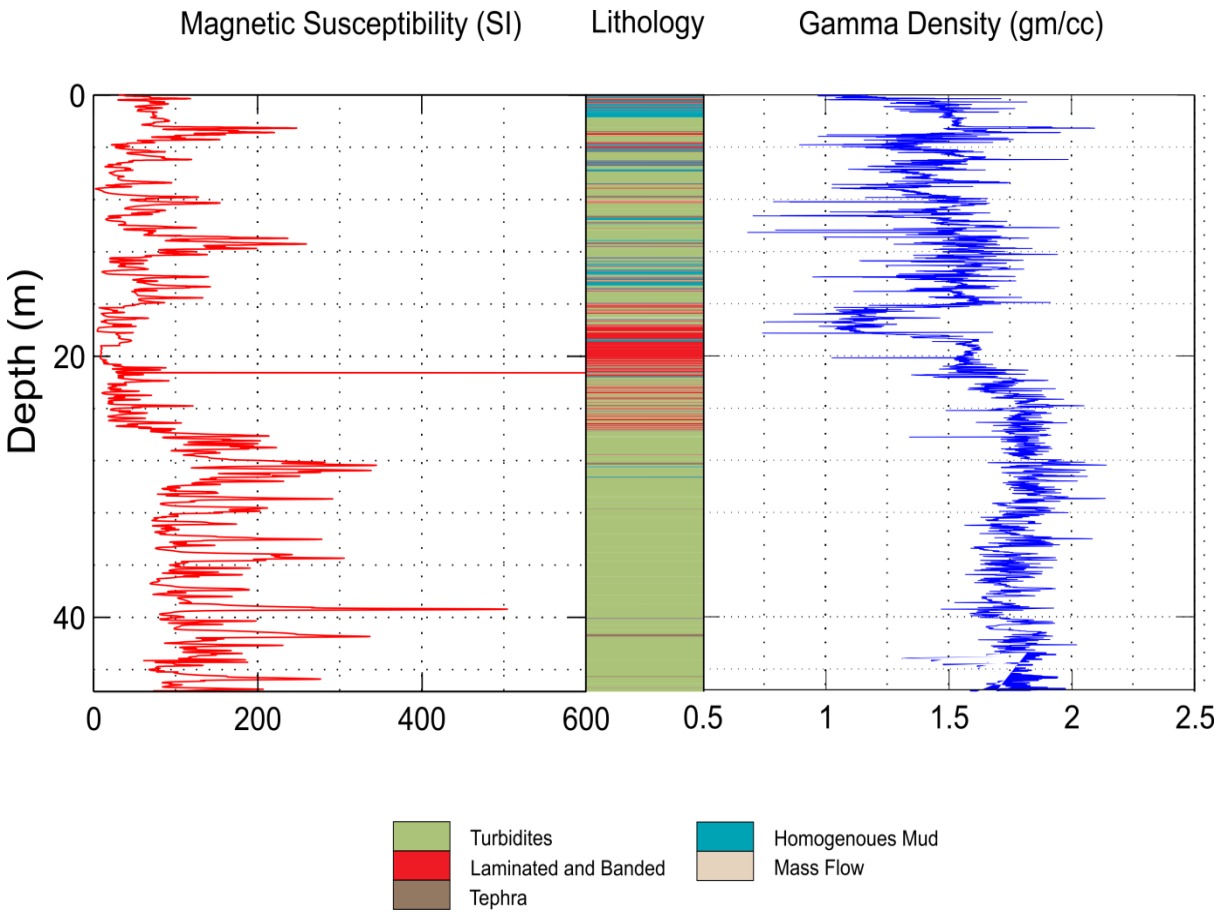

Fig. 3.1: Generalized stratigraphic section of the Northern Basin obtained from core description

d) Graded sand or silt (turbidite/homogenite): These units characterized graded sands at the base, followed upward by graded and laminated silt and homogenous mud. They typically have erosional contacts. Deposition of most of these units were triggered by earthquakes. The thicknes of the turbidite/homogenite units range from a few cm to 1.5 m. The main material for turbidites are generally volcanoclastic sediments.

e) Deformed lacustrine sediments and tephra layers: These sediments represent mass slides and slumps. They have thickness up to couple of meters and characterized by soft sediment deformation structures (disharmonic folds and faults), with a chaotic internal structure.

3.1.2 Age Model

Age model for Northern Basin stratigraphic section is established using three ^{14}C ages (Table 3.1), tephra ages (Sumita and Schmincke, 2011) (Table 3.2), and varve counting (Damcı and Çağatay, submitted) (Fig 3.1). Varve counting process is applied using a numerical radiography method and then using the ages tephra layers and the ages of the boundary of Marine Oxygen Isotope Stages (MIS) established by the oxygen isotope analysis.

Table 3.1: AMS 14C dating results, sample ID, composite depth, calibrated age

Site,Bore,Hole, Section	Core depth	Composite depth	14C age a. BP	Calibrated age a. BP
50341A1H1	97-99 cm	1.41 m	645±30	610±48
50341A5H2	9-11 cm	13.81 m	3880±45	4330±78
50341A11H1	8-9 cm	32.36 m	15300±45	18590±62

Table 3.2: Tephra ages that are used for age model for the last 26 ka in Northerm Basin stratiraphic section (tephra ages after Landmann, 1996, obtained by varve counting) .

Tephra ages (yr)	**Composite depth (m)**
1000*	2.87
2100*	4.23
2600*	7.85
4330*	13.81
6000*	16.76
6800*	17.61
7192	17.69
12500*	21.38
13500	23.725
13750*	28.178
18590*	32.36

Based on the established age model the various stratigraphic and climatic periods, such as Holocene, Younger Dryas, Bølling-Allerød, Late Glacial Maximum (LGM), can be distinguished on the studied Northern Basin stratigraphic section (Table 3.3).

Table 3.3: Different climate periods during the last 26 ka BP

Period	**Age interval (yr)**	**Sediment thickness (m)**
Holocene	11500 - 0	14.75
Younger Dryas	12800 - 11500	6.03
Bølling-Allerød	14700 - 12800	7.00
Deglaciation	18000 - 14700	2.36
LGM	20000 - 19000	6.15

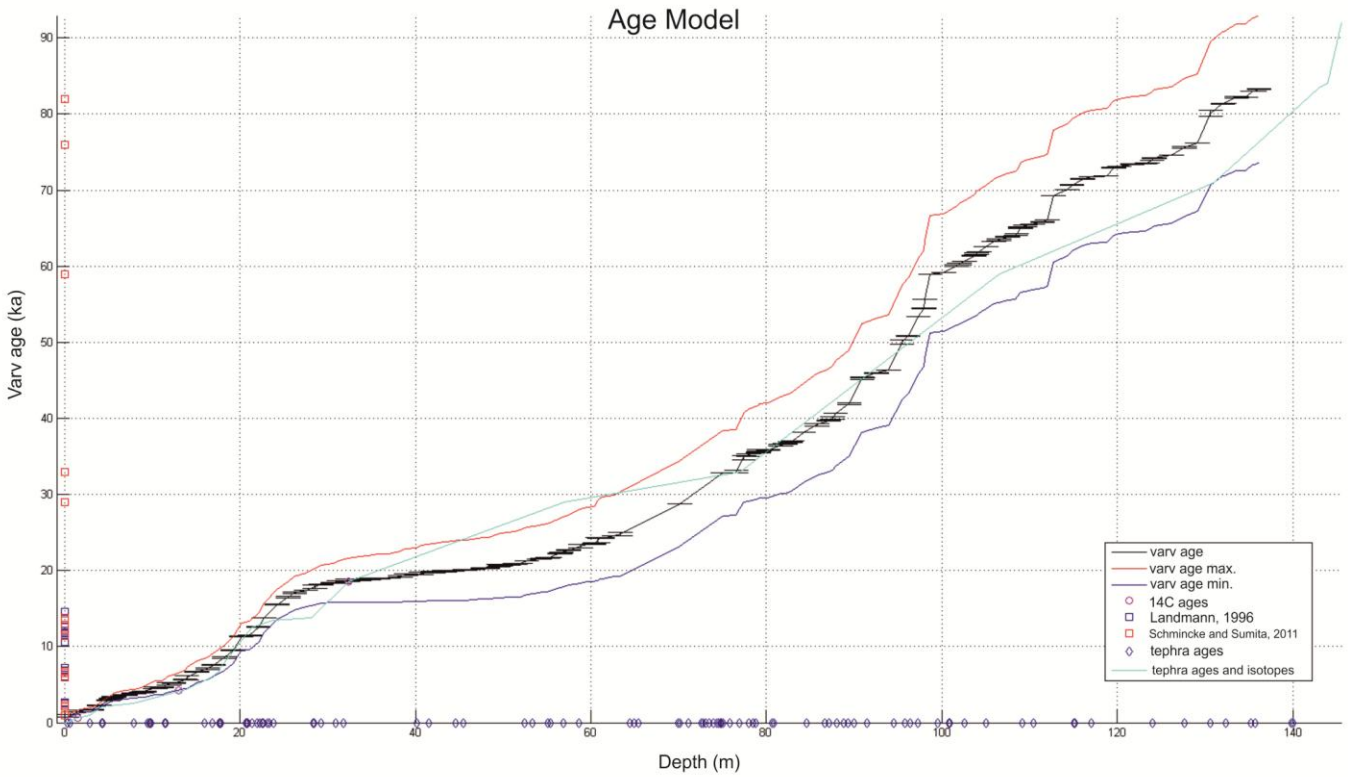

Fig 3.1: Age model based on tephra ages, ^{14}C ages, varv counting and isotopes

3.2 Geochemistry

To determine the biosphere-atmosphere interaction of the lake environment, several geochemical proxy analyses were performed, including TOC/TIC, stable isotope,, XRD and XRF Core scanner analyses. The results of these analyses are presented below.

3.2.1 TOC/TIC Values

TOC/TIC and stable isotope values of sediments in the Northern Basin stratigraphic section are given in Fig 3.2. The Holocene (MIS1) sediments contain high TOC values than the older sediments (26-11.5 ka BP). The highest TOC values (>4%) are seen in in the time intervals 4.9-4 ka BP, 6-5.5 ka BP and 7.8-6.4 ka BP. The highest TIC values occur during 4.8, 8.0-6.2, 8.9, 10.7 and 11.5 ka BP.

During the time interval between 26-15 ka BP, both TOC and TIC values decrease below 4%. The interval between 21.7-19.5 ka BP have some oscillating TOC and TIC values, which show negative correlation between them. Around 11.5 ka BP (end of Younger Dryas), significantly increased TIC value is measured (Fig 3.2). There is increase in TOC and TIC values in general during the Holocene with some oscillations. During the last 4 ka BP up to present, those TOC and TIC values show slight decrease. The degree of correlation between TOC and TIC C values are much lower and statistically in significant (r=0.005) during MIS-2 compared to MIS-1 (Holocene) (r=0.5).

3.2.2 Stable Oxygen and Carbon Isotope Values

Bulk carbonate stable oxygen and carbon analysis results of a total of 124 samples are shown in Fig 3.2. $\delta^{18}O$ values range between -6.2‰ and +4 ‰ PDB (standard deviation; σ=‰1.94) and $\delta^{13}C$ values vary between -3.5 ‰ and +5.1 ‰ PDB. There is a strong correlation between $\delta^{18}O$ and $\delta^{13}C$ (r>0.85) as shown in Fig 4.2.

The highest $\delta^{18}O$ are observed in 11.75 ka BP, 7-6 ka BP, 5-4 ka BP and 1- 0 ka BP. The highest $\delta^{13}C$ values are seen in similar periods as $\delta^{18}O$. During the period of 14-13 ka BP, relatively higher values of both $\delta^{13}C$ and $\delta^{18}O$ were measured than those in the periods before and after. The period from Pleistocene –Holocene transition at 11.5 to ~4 ka has high $\delta^{13}C$ values and mostly negative $\delta^{18}O$ values (Fig 3.2). Oscillating $\delta^{18}O$ and $\delta^{13}C$ isotope values are observed during the last 5 ka.

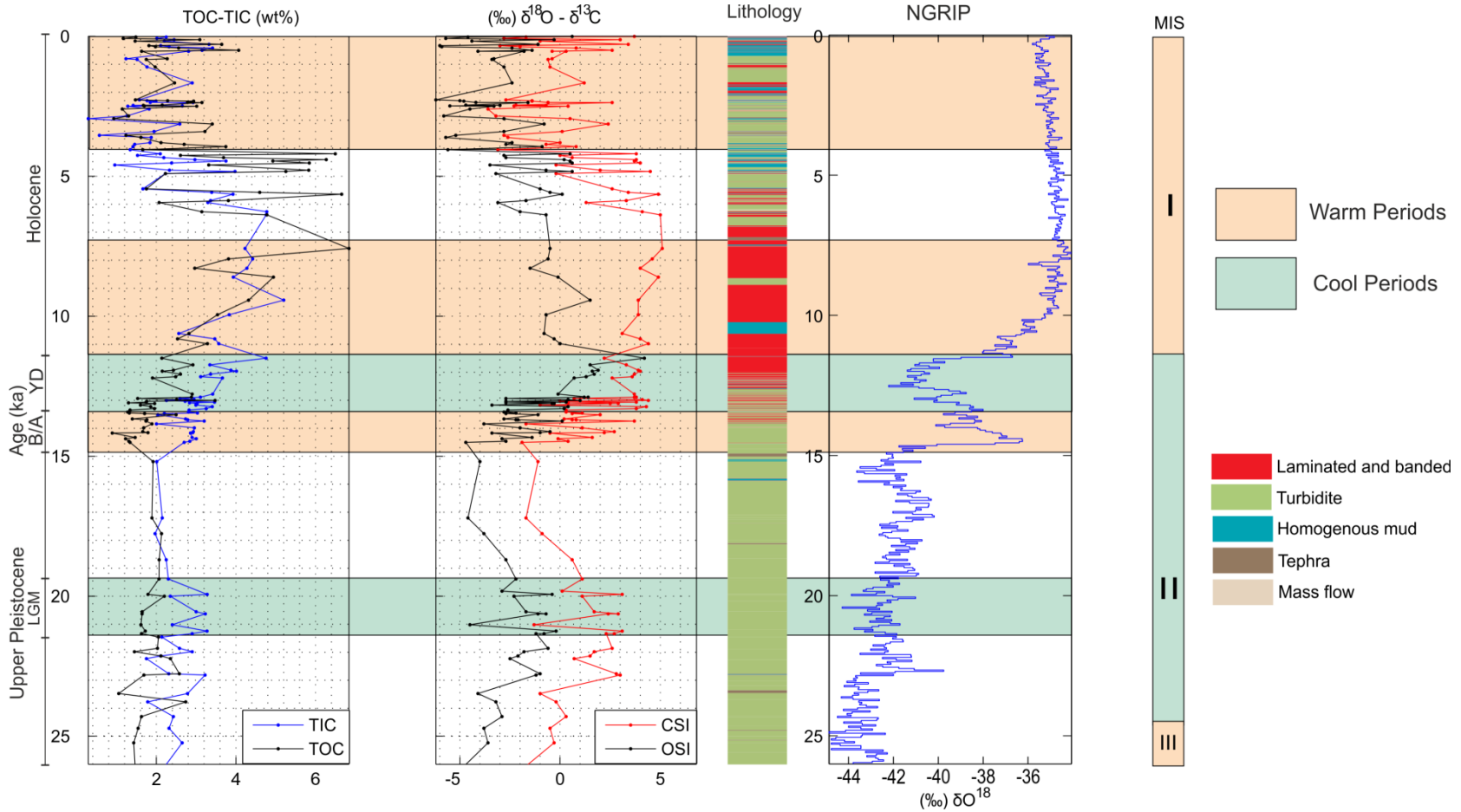

Fig 3. 2: Lithostratigraphy and proxy profiles of: TOC/TIC values, $\delta^{18}O$ and $\delta^{13}C$ values of bulk carbonate in Northern Basin stratigraphic section and correlation of $\delta^{18}O$ values of Northern Greenland ice core covering the last 26 ka calBP (Andersen et al., 2004)

3.2.3 XRD Results

A total 16 samples are analyzed to determine mineralogical composition of the sediments in the Northern Basin stratigraphic section in Lake Van. Distance from the shore of the drilling site (6 km) might allow autochthonous carbonate sedimentation in the basin.

In Lake Van sediments in 12-11.5 ka BP (Younger Dryas), there is a significant increase in dolomite shown in Fig 3.3 (see App A7). The part of the stratigraphic section around 4.5 ka BP also contains some dolomite, but at significantly lower amounts than in the interval of Younger Dryas. In the dolomite-bearing intervals aragonite shows marked depletion with very low dolomite/aragonite ratios. This may suggest aragonite transformation to dolomite. High calcite and low aragonite percentages are observed in the interval between 23-21 ka BP, corresponding to Late Glacial Maximum (LGM).

The intervals enriched in aragonite have the highest (heaviest) $\delta^{18}O$ values. There is a good correlation between aragonite and $\delta^{18}O$ values.

3.2.4 XRF Results

Profiles of XRF titanium (Ti), calcium (Ca) and iron (Fe) versus age of the stratigraphic section is given in Fig. 3.4. Ti, Zr and to a lesser extend Fe as proxies of detrital mineral input are more enriched in late Holocene sediments (last 5 ka) than in the earlier part of the Holocene and late Pleistocene sediments (Fig 3.4). Ti shows extreme depletion during the Younger Dryas (12.8-11.5 ka), but shows some enrichment during the Bølling-Allerød (14.5-12.8 ka). Ca as a proxy of carbonate sedimentation is enriched during the Younger Dryas and early Holocene and depleted in the Bolling-Allerod and Late Glacial sediments (MIS-2) (Fig. 3.4)

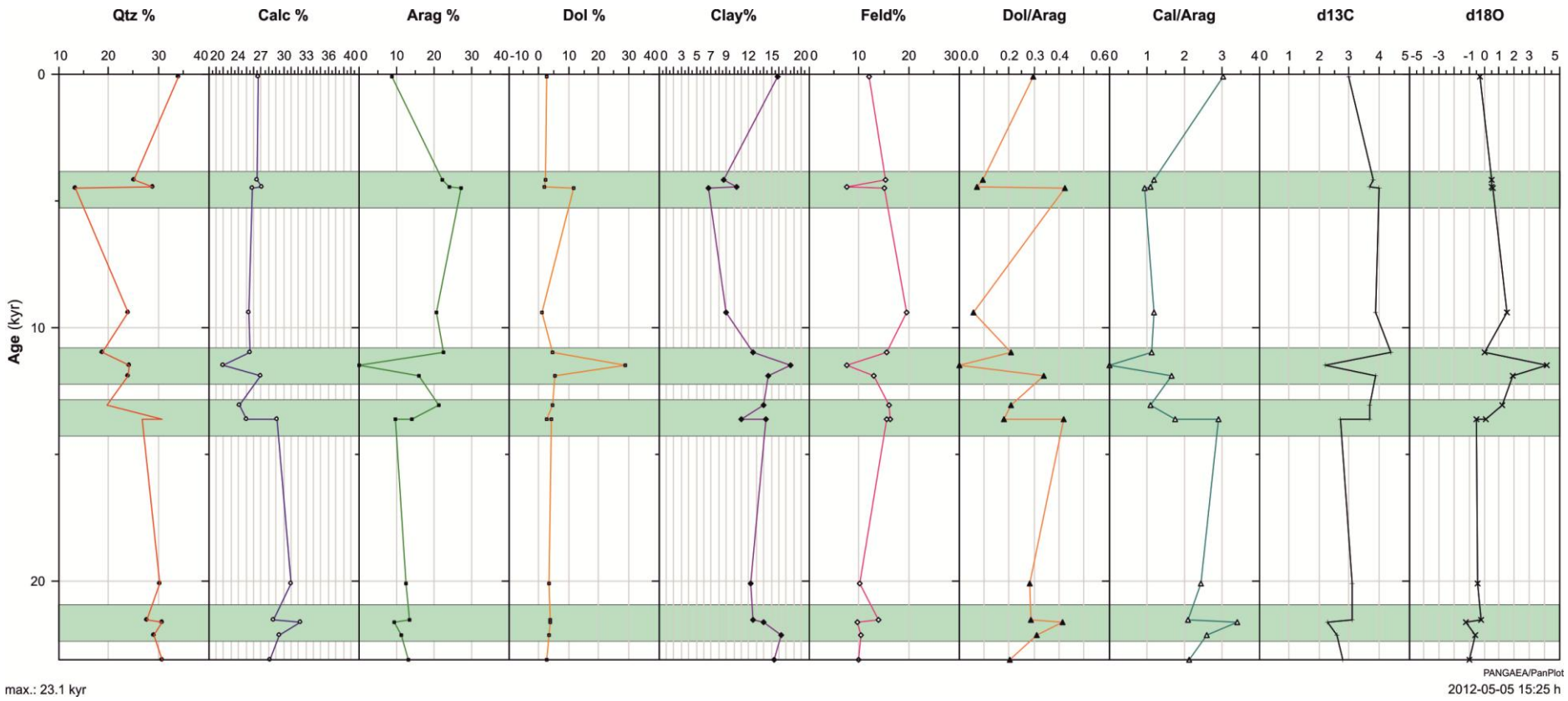

Fig 3. 3: Graphic of age versus mineral percentages, mineral ratios and stable isotope content of the Northern Basin sediments.

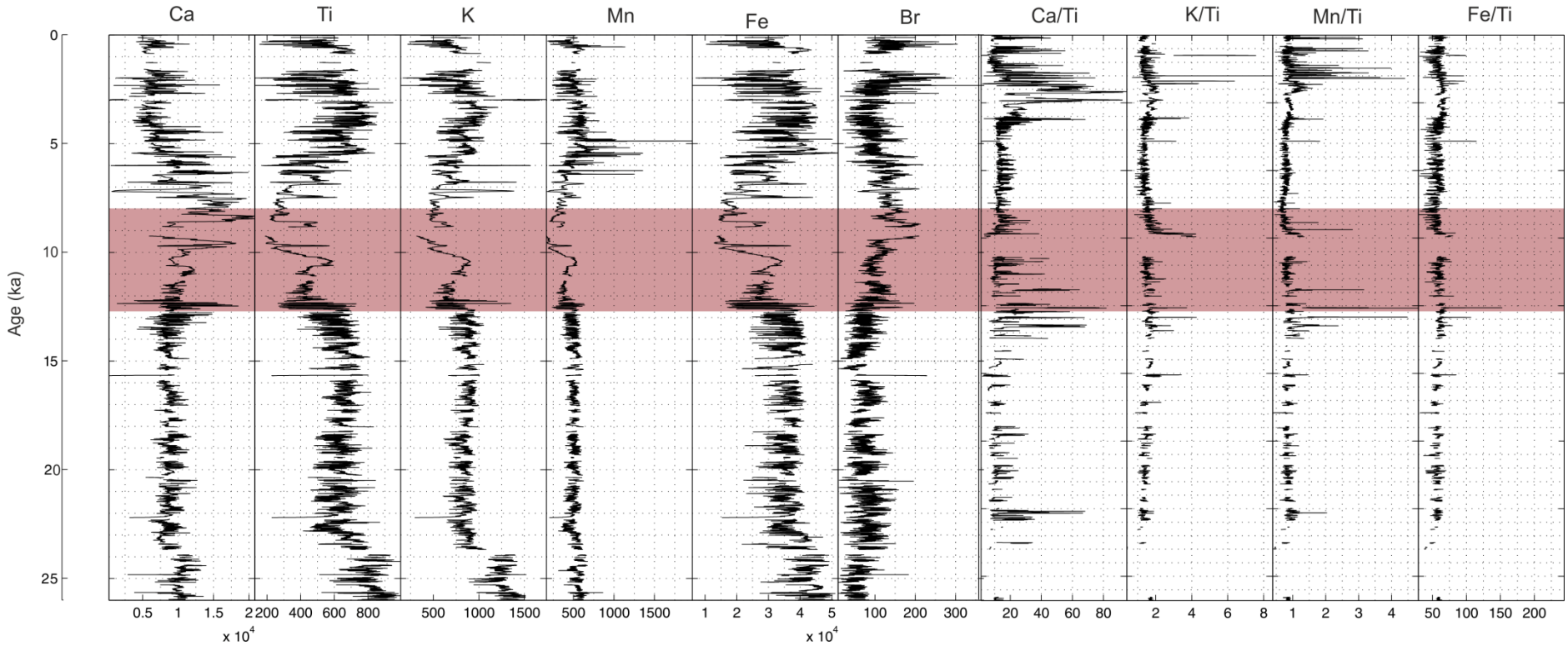

Fig 3. 4: XRF results of 26 ka BP

4. DISCUSSION

In this chapter, results of geochemical proxy analyses are discussed in terms of two headings: lake level changes and abrupt climate changes. In these contexts, especially stable isotope values, TOC/TIC results and XRD results are important (Fig 3.2, Fig 3.3).

4.1 Abrupt Climate Changes

Rapid lake level decline period from 12.8 ka BP to 11.5 ka BP, most probably corresponds to Younger Dryas and coincides with Pleistocene-Holocene transition. Low organic productivity and high isotope values during this period indicates that this was a cold and dry period. Mineralogical analyses show the presence dolomite, suggesting increased evaporation and high salinity with Mg/Ca ratio. XRF core scanner Ti and Fe profiles indicate low detrital input and thus low river activity during this period. The inverse correlation between stable carbon and oxygen isotope values and TOC and TIC values, all suggesting an abrupt climate change during the final stages of the Younger Dryas (Table 3.3). Moreover, low Ti and Fe suggest low detrital mineral input during the Younger Dryas and support dry conditions with high evaporation/precipitation.

The weak or negative correlation between TOC and TIC during most part of the MIS-2 suggests low degree of nutrient cycling and lake mixing and/or consistently low temperatures. During the Last Glacial Maximum (LGM) (Table 3.3) δ18O values oscillate between 0‰ and -3.5‰ which are higher values than the period between 26-22 ka BP indicating relatively dry climate conditions (Fig 3.2). It is indicated in the previous studies that Late Glacial period was represented by high aridity (Wick et al., 2003).

Bølling-Allerød (B/A) (14.7 -12.8 ka BP) event is represented by oscillating oxygen and carbon isotope values with higher amplitude than those in LGM (Fig 3.2). High δ13C values (>4‰) and relatively high TIC values (>3%) strongly suggest that this period was arid.

Lake van stable isotope records mostly show oscillations with a periodicity of about 1600 years (Fig 3.2), coinciding with 1470 ± 500 years cyclicity of the Dansgaard-Oeschger (D-O) events or the Bond events. Bond et al. (1997) argues that there is cyclicity in the Holocene climate with a periodicity of approximately every 1470 ± 500 years corresponding to rapid warming followed by gradual cooling. The D-O or Bond cyclicity in the Lake Van data is also

supported by the very strong correlation between the Lake Van isotope, TOC and TIC data and the Northern Greenland Ice Core (NGRIP) isotope data.

The last 4 ka is represented by some very low δ18O values (<-5‰) corresponding to wet periods. In Eastern Mediterranean at some different sites such as Frassino Lake in north Italy, similar depleted oxygen isotope record was obtained from molluscs indicating wetter climate period at 4 ka BP (Roberts et al., 2008). As indicated in previous studies in Lake Van and Eski Acıgöl (central Turkey) show isotope trends similar to Lake Zeribar (northwest Iran) records corresponding a wet climate in early Holocene (Jones and Roberts, 2008). The period between 6-4 ka BP is indicated as climatic optimum in Lake Van area (Wick et al., 2003). During 5-4 ka BP δ18O values in Lake Van are relatively high and oscillating compared to the adjacent periods before and after. This climate shift during 5-4 ka BP is known as "Holocene 3 Event", and is believed to the cause of the collapse of dry farming agricultural system (Wenxiang and Tungsheng, 2004).

4.2 Lake Level Changes

In closed lake basins TOC, TIC, δ18O and δ13C values show strong correlation (Li and Ku, 1997) (Fig 4.2). Relationship between $\delta^{18}O$ and $\delta^{13}C$ in terminal lakes is a function of paleohydrological changes, evaporation, organic productivity in the lake and total carbonate concentration. Positive covariance between $\delta^{18}O$ and $\delta^{13}C$ values of lake sediments in lakes is common in those that are remained as closed basins for more than 5000 years (Fig 4.2) (Li and Ku, 1997). Enhanced evaporation/precipitation ratio results in increased $\delta^{18}O$ values in deposited carbonate. However, it should be noted that, covariance between stable isotopes becomes weaker if the lake level remains stable for a long time because of evaporation/productivity effect.

The other important factor that controls oxygen isotope values is the temperature of the lake water (Hyas and Grossman, 1991). This relation is explained by the Epstein equation:

$$T = 16.5 - 4.3\,(\delta^{18}O_c - \delta^{18}O_w) + 0.14\,(\delta^{18}O_c - \delta^{18}O_w)^2$$

where T: temperature; $\delta^{18}O_c$: oxygen isotope in carbonate; $\delta^{18}O_w$: oxygen isotope in lake water. This equation indicates inverse relation between temperature of the

carbonate precipitation and the $\delta^{18}O_c$ values of the precipitating carbonate (Epstein et al., 1953). This relation corresponds to 5°C per $\delta^{18}O$ ‰ unit. However, in closed basins $\delta^{18}O$ values are more influenced from evaporation/precipitation ratio than temperature in water column, whereas $\delta^{13}C$ values are controlled by both organic productivity and evaporation (Li and Ku, 1997; Roberts et al., 2008). As a result, relation between the stable isotope values and TOC (organic productivity) / TIC (inorganic carbon content) show significant correlation with climate changes.

In closed basin lakes, like Lake Van, positive correlation of $\delta^{18}O$ and $\delta^{13}C$ values depends on several paleohydrological controlling factors such as evaporation/precipitation ratio, buffering effect of total CO_2 on $\delta^{13}C$, and organic productivity (TOC). These relations can be summarized as the following (Li and Ku, 1997):

1) *Effect of hydrological balance:* even a little change in alkalinity ($\sum CO_2$) of lake water by mixing of fresh water input by rivers with the lake water will cause strong covariance between stable isotope values during volume change due to the dilution effect. Fresh water input to the lake will reduce the $\delta^{18}O$ and $\delta^{13}C$ values of the lake water as well as the salinity and carbonate alkalinity. This alkalinity difference between the Lake Van water and river water was measured in previous studies as ~150 mmol/l ($A_{lake\ water}$= 155 mmol/l, A_{river}=0.64-3.44 mol/) (Reimer et al., 2009). As the alkalinity value of the input water becomes similar to the lake water alkalinity, similarity and the covariance between between $\delta^{18}O$ and $\delta^{13}C$ increase. The difference can be calculated by the following formula:

$$\delta_{mw} = \delta_{lw} \cdot f_{lw} + \delta_{rw} \cdot f_{rw}$$

δ_{lw} :isotope value of lake water; δ_{rw}: isotope value of river water; f_{lw}: fraction of lake water in mixture; f_{rw}:fraction of river water in mixture

2) *Effect of vapor exchange:* Vapor exchange between the lake and the atmosphere water forces the stable isotope values to stay in steady-state levels as the lake level is stabilized. As a result the signal between the isotope values becomes weaker.
3) *Effect of evaporation and organic productivity:* As the evaporation increases, ^{16}O becomes enriched in the vapor phase, and the heavy isotope becomes increased in the lake water. High evaporation will cause a drop in lake level volume because related to intense evaporation, there will be less input of fresh water to the lake and ^{18}O and ^{13}C values will increase. Sharp drop of lake level induced by high evaporation will cause

degassing of CO_2, and enhanced organic productivity in association with vertical mixing of the lake water. As a result, both isotope values will be enhanced related to rapid lake level drop due to evaporation increase giving strong correlation between $\delta^{18}O$ and $\delta^{13}C$ as seen in Lake Van Holocene sediments (Fig 4.2).

4) *Effect of alkalinity change:* Covariance between the stable isotope values also might be the function of alkalinity ($\sum C O_2$) change in the lake water with time. Assuming the total alkalinity of the lake water is stabilized, weaker $\delta^{18}O$ and $\delta^{13}C$ covariant trends would be accompanied with higher $\sum CO_2$ values.

To determine the climatic changes in Lake Van, those factors were taken account. For a proper determination, following measurements must be considered: in Lake Van the oxygen isotope ratio of atmospheric moist is -21.04‰ SMOW / 15°C (Schoell and Faber, 1978). The calculated value of $\delta^{18}O$ of Lake Van sediments is 0.93 ‰ PDB, the measured value of $\delta^{18}O$ in present day carbonate is 0.78 ‰ PDB (Lemcke and Sturm, 1997).

Considering the above information about closed lake basins, strong positive correlation (r>0.85) between stable isotope values indicates that Lake Van remained as a closed basin in general as shown in Fig 4.2. Cross-plots of different parameters such as TOC, TIC, $\delta^{18}O$ and $\delta 1^{3}C$ also show strong correlation between organic productivity, inorganic carbon accumulation, evaporation/precipitation and lake hydrology (Fig 3.2, Fig 4.2).

Highest $\delta^{18}O$ values are observed in time period between 12.5-11.5 ka BP corresponding to the Younger Dryas. This period must have associated with very low lake levels (Fig 3.2). The lowest $\delta^{18}O$ values (<-4‰) are seen during 4-2 ka BP, 17-14 ka BP and 21.3 ka BP that most probably corresponds to relatively high lake levels.

According to oxygen stable isotope values the terms corresponding to high lake levels (17-14 ka BP) also refer to lake water stratification and related to this weakened nutrient cycle and less organic productivity. Rapid lake level drop which began around 13.8 ka BP, reached its lowest levels in 12.5-11.5 ka BP. Stable isotope values show high amplitude oscillations during 13.8-13 ka BP. In the period of 14-

11.5 ka BP which corresponds to low lake levels, show parallel increase in TOC and TIC values (Fig 3.2). By contrast with the generally strong positive correlation between $\delta^{18}O$ and $\delta^{13}C$ values for the whole of the Northern Basin sedimentary section, a negative correlation between $\delta^{18}O$ and $\delta^{13}C$ values is observed during the late part of the Younger Dryas (around 11.5 ka BP) (Fig 3.2). This rapid drop of lake level during 11.5 ka is supported by precipitation of high amount of dolomite in the lake sediments (see App A7, Fig 3.3). This marked lake level drop appears to have influenced the organic productivity negatively. Moreover, low Ti and Fe suggest low detrital mineral input during the Younger Dryas, supporting dry conditions with high evaporation/precipitation and a significantly low lake level.

The correlation between the TOC and TIC also reverses from highly significant positive values during the Holocene (MIS-1) to insignificant, or negative values during the late Pleistocene (MIS-2), suggesting considerable change in the hydrology and biogeochemical cycling at the transition from the late Pleistocene to Holocene. The weak or negative correlation between TOC and TIC during most part of the MIS-2 suggest low degree of nutrient cycling and lake mixing and/or low temperatures.

$\delta^{18}O$ and $\delta^{13}C$ values showing oscillating, but decreasing trend from 11.5 ka BP up to 2.5 ka BP, indicating in general an increasing lake level until about 2.5 ka BP. The amplitude of oscillations during 4.5-2 ka BP in a similar way to those during 14-13 ka BP (Bolling-Allerod). During these periods of rising lake level, TOC values show a decline.

Our results regarding the lake level changes are in general agreement with the results of previous studies based on sediment cores from the lake (Landmann et al., 1996a; Landmann et al., 1996b; Reimer et al., 2009; Roberts et al., 2010) and the ages of high stand terraces exposed above the lake level (Kuzucuoğlu et al., 2010).

Kuzucuoğlu et al. (2010) states that there are two significantly high lake levels with altitude of 1700-1705 m that are climatologically controlled between 26-24.5 ka BP and 21-20 ka BP (Fig 4.1). In addition, (Kempe et al., 2002) point out a synchronous sedimentation of Engil River terrace which is 80 m above today's lake level associated with transgression of 21.3 ka BP. We also have corraletable data corresponding to these periods that are represented by low $\delta^{18}O$ and $\delta^{13}C$ values (Fig 3.2).

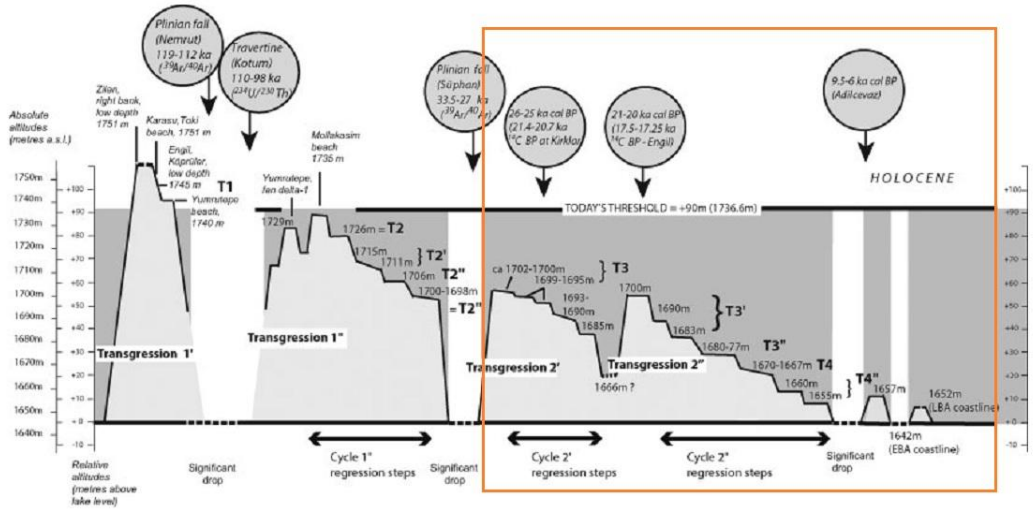

Fig 4. 1: Synthetic curve of Lake Van level changes from Kuzucuoğlu et al. (2010).

There are also differences in between our study results and previous studies. The very low lake level or dry lake during 16-15 ka BP proposed by Landmann et al. (1996a, b) and Reimer et al. (2009) is not supported by our data. Instead, our data show relatively high lake levels during that period (Fig 3.2).

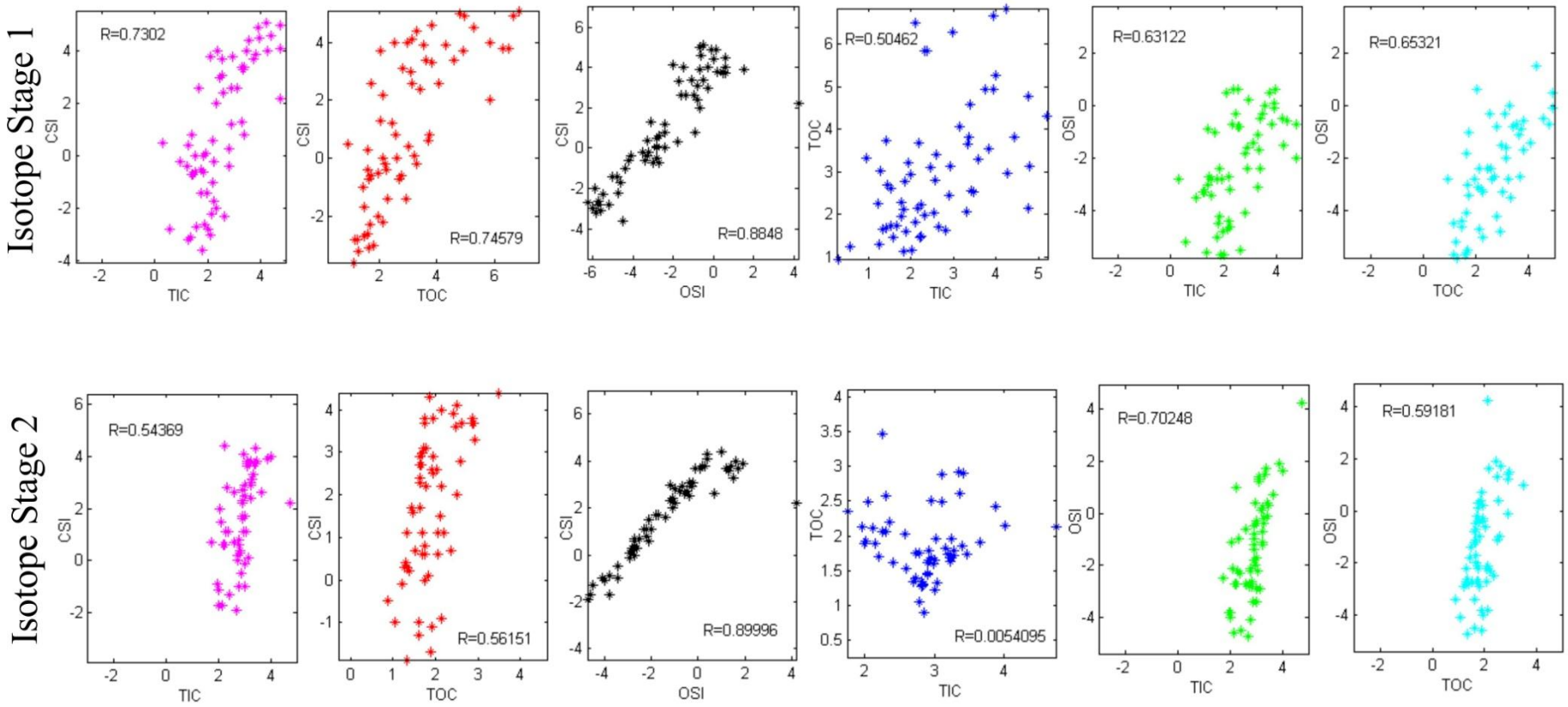

Fig 4.2:Cross plots and correlation coefficients of different parameters of Lake Van

5. CONCLUSIONS

Lake Van, situated on the East Anatolian Plateau and between different mid-latitude climate systems, is in an excellent location for continental paleoclimatological studies. Multi-proxy analyses of ICDP bore-hole cores from the Northern Basin (NB) of Lake Van have produced important paleoclimatic and paleoenvironmental data.

The NB composite sedimentary section observed in the ICDP boreholes consists of basically 5 main lithological types: a) banded and/or laminated clayey silt, b) homogeneous clayey silt, c) tephra, d) graded sand-silt (turbidite-homogenite), and e) deformed lacustrine sediments and tephra layers. Laminated and banded mud layers and homogenous gray muds are the normal, background sediments of the lake. The laminated sediments consist of varves representing seasonally deposited laminae.

The rapid climate changes in Lake Van are mainly controlled by the North Atlantic Oscillation (NAO). Rapid changes in negative North Atlantic Oscillation (NAO) that brings colder and dryer air mass or positive NAO that brings wetter and warmer air mass appear to have been particularly important in the climate and the corresponding evaporation/ precipitation ratio. In Lake Van, the bulk carbonate is enriched in the light isotopes during the last 4 ka BP, suggesting a warm and wet climate that was probably controlled by positive NAO (McIvor, 2010). During this period high precipitation/evaporation ratio caused the lake level to increase. This in turn resulted in stronger water stratification, keeping the organic productivity at relatively low levels, as indicated by relatively light carbon isotope values. The period between 5 and 4 ka BP was particularly a dry and warm, as indicated by heavy oxygen and carbon isotopes and presence of dolomite (12%). This period is also characterized by high organic productivity, associated with low lake level and availability of nutrients from the hypolimnion. Possibly the Mediterranean climate, which is the subtropical high pressure system with hot and dry summers and cold and wet winters, was effective during 5-4 ka BP.

Dry and cold period of Younger Dryas (YD) at the transition from the Pleistocene to Holocene, which characterized by significant changes in the thermohaline circulation of North Atlantic (Brauer et al., 2008), is well represented in Lake Van sedimentary record. YD in Lake Van is represented by extreme aridity in Lake Van records, which is indicated by the maximum oxygen isotope values and large amount of dolomite (30%). All geochemical proxies indicate high evaporation, significantly low lake levels and high salinity during the YD.

The Bølling-Allerød (B/A) period is represented by very high oscillations and instability in most of the proxies that indicate increasing warm and dry conditions with high variability under the influence of NAO (Seager and Battisti, 2007).

During the last glacial maximum, the oxygen and carbon isotope values are low, ranging between -4.5-0 ‰ and -1.5-3 ‰, respectively. TOC values are low (1.5%) and the main carbonate in the sediments is calcite (32%). All these proxy data indicate relatively high precipitation/evaporation ratio and lake levels and lower salinity than today. During the cold and dry LGM period, negative NAO was the predominant climate system in the region (McIvor, 2010).

The variability in the stable isotope data appears to indicate D-O and Bond cyclicity, suggesting climate change with approximately 1500 year periodicity. However, to determine the periods in the data, spectral analyses should be made as part of future studies. Micro- and nano-paleontological analysis (such as nano-fossils, diatoms and pollens) are needed for further climate change studies in the Lake Van sediments. Furthermore, to distinguish the primary sedimentological and diagenetic mineral deposition, scanning electron microscope studies on carbonate minerals should be performed.

BIBLIOGRAPHY

Akçar, N., and Schlühter, C., 2005, Palaeoglaciations in Anatolia: a schematic review and first results.: *Eiszeitalter und Gegenwant*, v. 55, p. 102-121.

Allégre, C. J., 2008, Isotope Geology, Cambridge University Press.

Andersen, K. K., Azuma, N., Barnola, J. M., Bigler, M., Biscaye, P., Caillon, N., Chappellaz, J., Clausen, H. B., DahlJensen, D., Fischer, H., Fluckiger, J., Fritzsche, D., Fujii, Y., Goto-Azuma, K., Gronvold, K., Gundestrup, N. S., Hansson, M., Huber, C., Hvidberg, C. S., Johnsen, S. J., Jonsell, U., Jouzel, J., Kipfstuhl, S., Landais, A., Leuenberger, M., Lorrain, R., Masson-Delmotte, V., Miller, H., Motoyama, H., Narita, H., Popp, T., Rasmussen, S. O., Raynaud, D., Rothlisberger, R., Ruth, U., Samyn, D., Schwander, J., Shoji, H., Siggard-Andersen, M. L., Steffensen, J. P., Stocker, T., Sveinbjornsdottir, A. E., Svensson, A., Takata, M., Tison, J. L., Thorsteinsson, T., Watanabe, O., Wilhelms, F., White, J. W. C., and Project, N. G. I. C., 2004, High-resolution record of Northern Hemisphere climate extending into the last interglacial period: Nature, v. 431, no. 7005, p. 147-151.

Becker, J. S., 2002, State-of-the-art and progress in precise and accurate isotope ratio measurements by ICP-MS and LA-ICP-MS - Plenary Lecture: Journal of Analytical Atomic Spectrometry, v. 17, no. 9, p. 1172-1185.

Bisson, W., 2012, CCP14, Volume 2012: http://www.ccp14.ac.uk/about.htm.

Brauer, A., Haug, G. H., Dulski, P., Sigman, D. M., and Negendank, J. F. W., 2008, An abrupt wind shift in western Europe at the onset of the Younger Dryas cold period: Nature Geoscience, v. 1, no. 8, p. 520-523.

D'Arrigo, R., Jacoby, G., Wilson, R., and Panagiotopoulos, F., 2005, A reconstructed Siberian High index since A. D. 1599 from Eurasian and North American tree rings: Geophysical Research Letters, v. 32, no. 5.

Degens, E. T., **Wong, H. K.**, **Kempe, S.**, and **Kurtman, F.**, 1984, A Geological Study of Lake Van, Eastern Turkey: *Geologische Rundschau*, v. **73**, no. 2, p. 701-734.

Epstein, S., Buchsbaum, R., Lowenstam, H. A., and Urey, H., 1953, Revised carbonate-water isotopic temperature scale: Geological Society of America Bulletin, v. 64, p. 1315-1326.

Erinç, S., 1953, Doğu Anadolu Coğrafyası, İstanbul, İst. Üniv. Yay., v. 15, 60-79 p.:

GeoTek, 2012, MSCL Systems, Volume 2012, http://www.geotek.co.uk/products/mscl-s.

Hyas, P. D., and Grossman, E. L., 1991, Oxygen isotopes in meteoric calcite cements as indicators of continental paleoclimate: Geology, v. 19, p. 441-444.

Kadioglu, M., Sen, Z., and Batur, E., 1997, The greatest soda-water lake in the world and how it is influenced by climatic change: Annales Geophysicae-Atmospheres Hydrospheres and Space Sciences, v. 15, no. 11, p. 1489-1497.

Kempe, S., Degens, E.T., 1978, Lake Van varve record: the past 10,420 years, *in* Degens, E. T., Kurtman, F, ed., Geology of Lake Van: Ankara, Turkey, MTA Press, p. 9.

Kempe, S., Landmann, G., and Müller, G., 2002, A floating varve chronology from the last glacial maximum terrace of Lake Van/Turkey, Research in deserts and mountains of Africa and Central Asia, Volume 126: Berlin, p. 97–114.

Landmann, G., Reimer, A., and Kempe, S., 1996, Climatically induced lake level changes at Lake Van, Turkey, during the Pleistocene/Holocene transition: Global Biogeochemical Cycles, v. 10, no. 4, p. 797-808.

Lemcke, G., and Sturm, M., 1997, Third Millennium BC Climate Change and Old World Collapse, *in* Dalfes, N., Kukla, G., and Weiss, H., eds., NATO ASI Series, Volume 49: Berlin, p. 653-678.

Li, H. C., and Ku, T. L., 1997, $\delta^{13}C$-$\delta^{18}O$ covariance as a paleohydrological indicator for closed-basin lakes: Palaeogeography Palaeoclimatology Palaeoecology, v. 133, no. 1-2, p. 69-80.

Litt, T., Krastel, S., Sturm, M., Kipfer, R., Oercen, S., Heumann, G., Franz, S. O., Uelgen, U. B., and Niessen, F., 2009, 'PALEOVAN', International Continental Scientific Drilling Program (ICDP): site survey results and perspectives: Quaternary Science Reviews, v. 28, no. 15-16, p. 1555-1567.

McIvor, S., 2010, North Atlantic Oscillation: Past and Present, with case studies for 6Ka, 12Ka and 3Ma: Earth & E-nvironment, v. 5, p. 99-152.

Petschick, R., 2000, MacDiff 4.1.2 Manual.

Reimer, A., Landmann, G., and Kempe, S., 2009, Lake Van, Eastern Anatolia, Hydrochemistry and History: Aquatic Geochemistry, v. 15, no. 1-2, p. 195-222.

Reimer, P. J., Baillie, M. G. L., Bard, E., Bayliss, A., Beck, J. W., Bertrand, C. J. H., Blackwell, P. G., Buck, C. E., Burr, G. S., Kirsten, B. C., Damon, P. E., Edwards, R. L., Fiarbanks, R. G., Friedrich, M., Guilderson, T. P., Hogg, A. G., Hughen, K. A., Kromer, B., McCormac, G., Manning, S., Ramsey, C. B., Reimer, R. W., von der Plicht, J., and Weyhenmeyer, C. E., 2004, INTCAL04 Terrestrial radiocarbon age calibration, 0–26 cal kyr BP: Radiocarbon, v. 46, no. 3, p. 1029-1058.

Roberts, N., Jones, M. D., Benkaddour, A., Eastwood, W. J., Filippi, M. L., Frogley, M. R., Lamb, H. F., Leng, M. J., Reed, J. M., Stein, M., Stevens, L., Valero-Garces, B., and Zanchetta, G., 2008, Stable isotope records of Late Quaternary climate and hydrology from Mediterranean lakes: the ISOMED synthesis: Quaternary Science Reviews, v. 27, no. 25-26, p. 2426-2441.

Schoell, M., and Faber, E., 1978, New isotopic evidence for the origin of the Red Sea brines: Nature, v. 275, p. 436-438.

Seager, R., and Battisti, D. S., 2007, Challenges to our understanding of the general circulation: abrupt climate change., *in* Schneider, T., and Sobel, A. S., eds., The Global Circulation of the Atmosphere: Phenomena, Theory, Challenges., Princeton University Press, p. 331-371.

Sengör, A. M. C., Özeren, M. S., Keskin, M., Sakinç, M., Özbakir, A. D., and Kayan, I., 2008, Eastern Turkish high plateau as a small Turkic-type orogen: Implications for post-collisional crust-forming processes in Turkic-type orogens: Earth-Science Reviews, v. 90, no. 1-2, p. 1-48.

Sieger, R., 1888, Die Schvvankungen der hoch-armenischen Seen seit 1800 in Vergleichung mit einigen verwandten Erscheinungen.: Mitt K K Geogr. Ges., v. 95-115, no. 159-181, p. 390-426.

Stockhecke, M., Anselmetti, F. S., Meydan, A. F., Odermatt, D., and Sturm, M., 2012, The annual particle cycle in Lake Van (Turkey): Palaeogeography, Palaeoclimatology, Palaeoecology, v. 333-334, p. 148–159.

Sumita, M., and Schmincke, H. U., Volcanic, compositional and temporal evolution of dominantly Nemrut., *in* Proceedings 1st PaleoVan Workshop, Zurich, Switzerland, 2011.

Visbeck, M. H., Hurrell, J. W., Polvani, L., and Cullen, H. M., 2001, The North Atlantic Oscillation: Past, present, and future: Proceedings of the National Academy of Sciences of the United States of America, v. 98, no. 23, p. 12876-12877.

Wick, L., Lemcke, G., and Sturm, M., 2003, Evidence of Lateglacial and Holocene climatic change and human impact in eastern Anatolia: high-resolution pollen, charcoal, isotopic and geochemical records from the laminated sediments of Lake Van, Turkey: Holocene, v. 13, no. 5, p. 665-675.

APPENDICES

APPENDIX A1: XRD diffractogram of samples from 0.25 m

APPENDIX A2: XRD diffractogram of samples from 13.48 m

APPENDIX A3: XRD diffractogram of samples from 14.12 m

APPENDIX A4: XRD diffractogram of samples from 14.28 m

APPENDIX A5: XRD diffractogram of samples from 18.39 m

APPENDIX A6: XRD diffractogram of samples from 19.09 m

APPENDIX A7: XRD diffractogram of samples from 19.5 m

APPENDIX A8: XRD diffractogram of samples from 20.1 m

APPENDIX A9: XRD diffractogram of samples from 22.44 m

APPENDIX A10: XRD diffractogram of samples from 25.47 m

APPENDIX A11: XRD diffractogram of samples from 26.61 m

APPENDIX A12: XRD diffractogram of samples from 34.65 m

APPENDIX A13: XRD diffractogram of samples from 37.04 m

APPENDIX A14: XRD diffractogram of samples from 37.21 m

APPENDIX A15: XRD diffractogram of samples from 38.22 m

APPENDIX A16: XRD diffractogram of samples from 40.05 m

Fig A1: XRD diffractogram of samples from 0.25 m

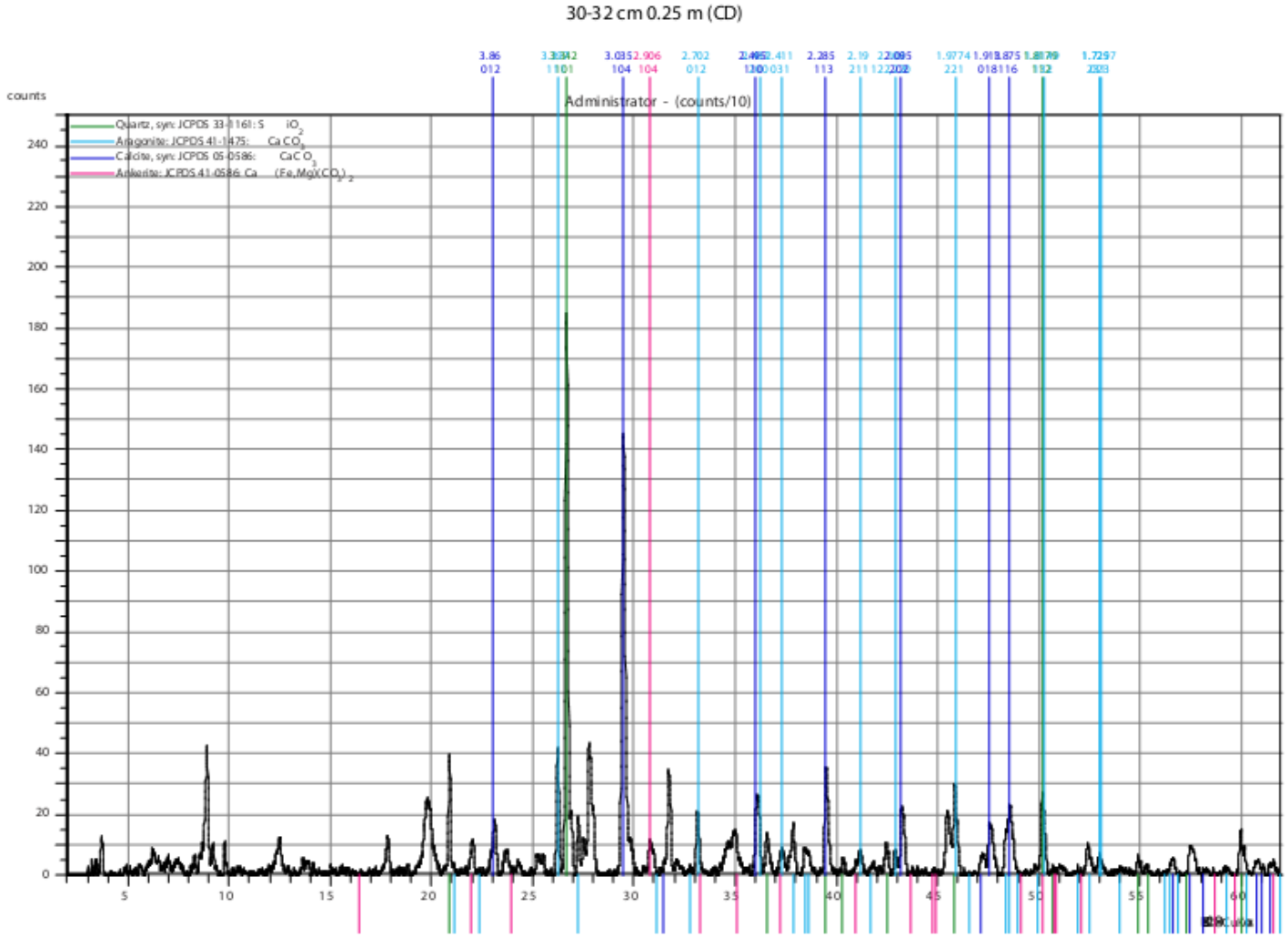

Fig A2: XRD diffractogram of samples from 13.48 m

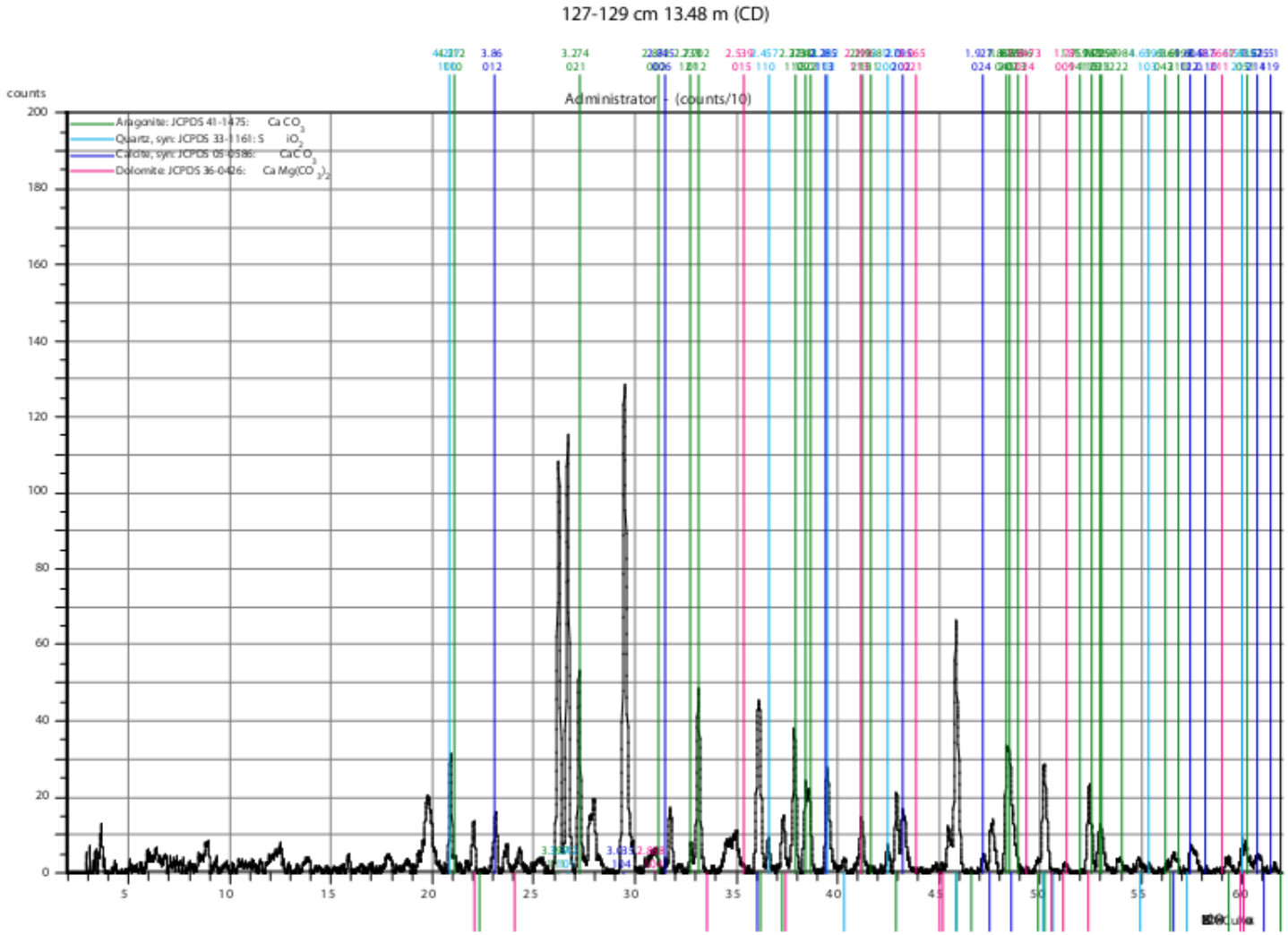

Fig A3: XRD diffractogram of samples from 14.12 m (CD)

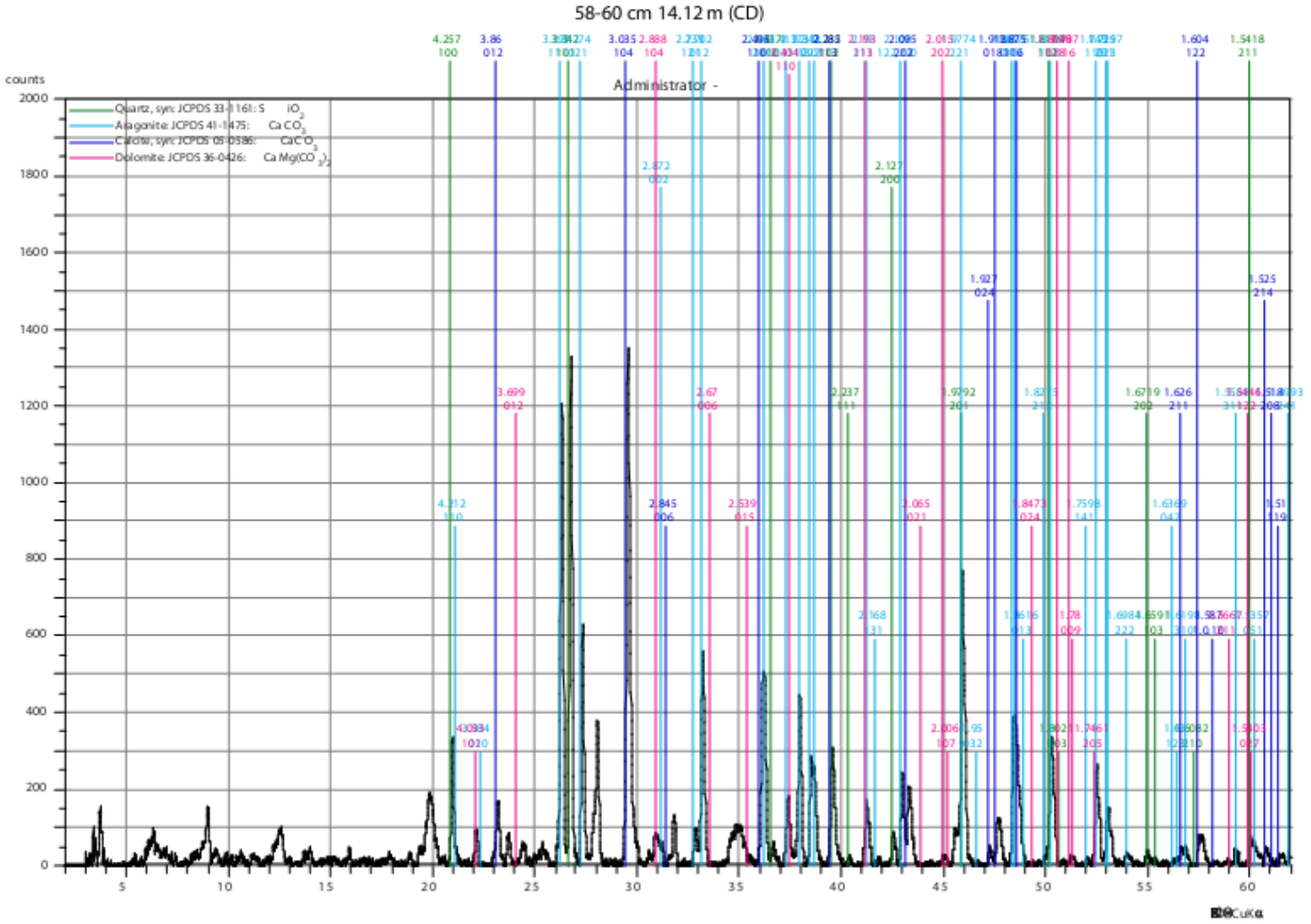

Fig A4: XRD diffractogram of samples from 14.28 m

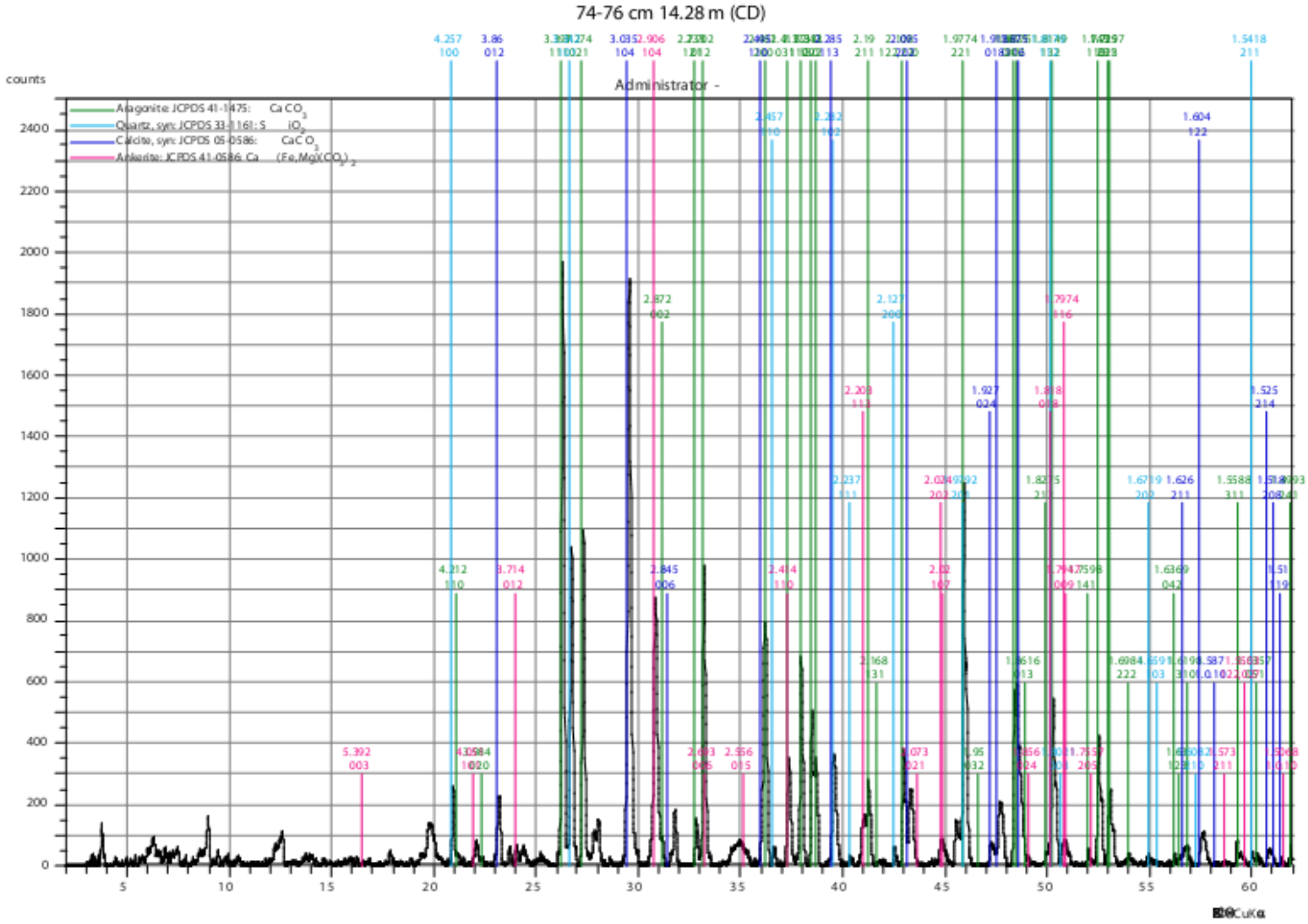

Fig A5: XRD diffractogram of samples from 18.39 m

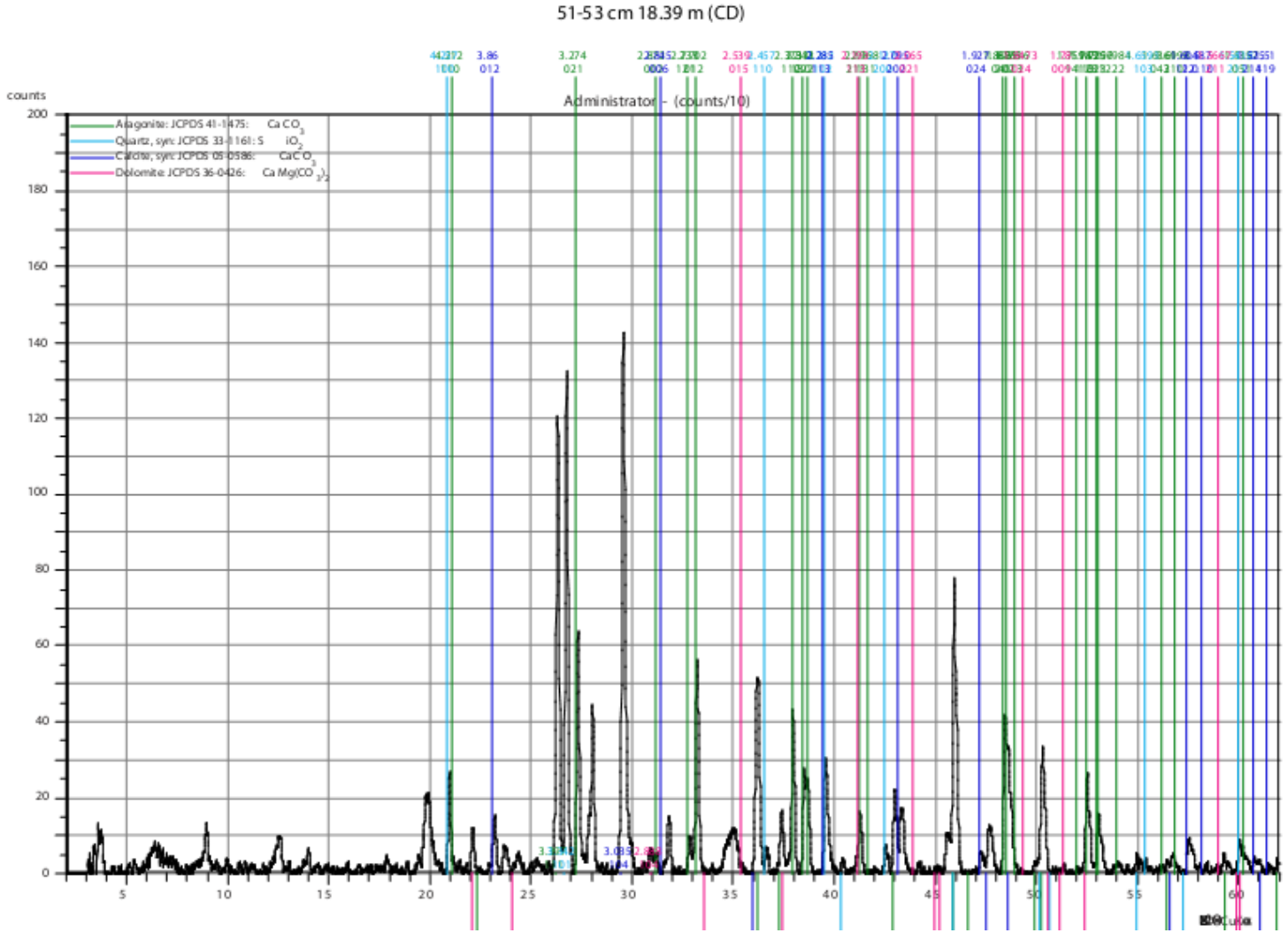

Fig A6: XRD diffractogram of samples from 19.09 m

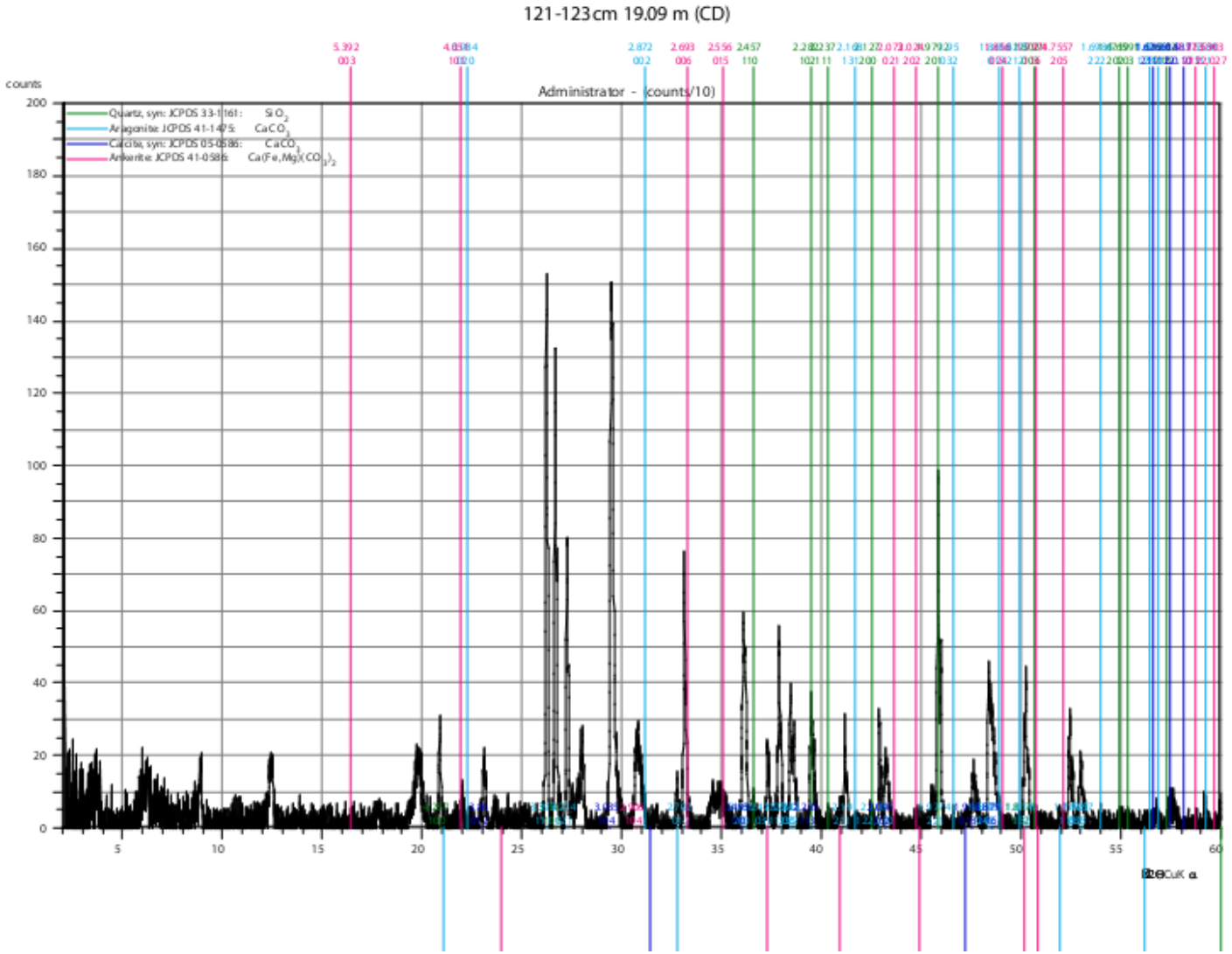

Fig A7: XRD diffractogram of samples from 19.5 m

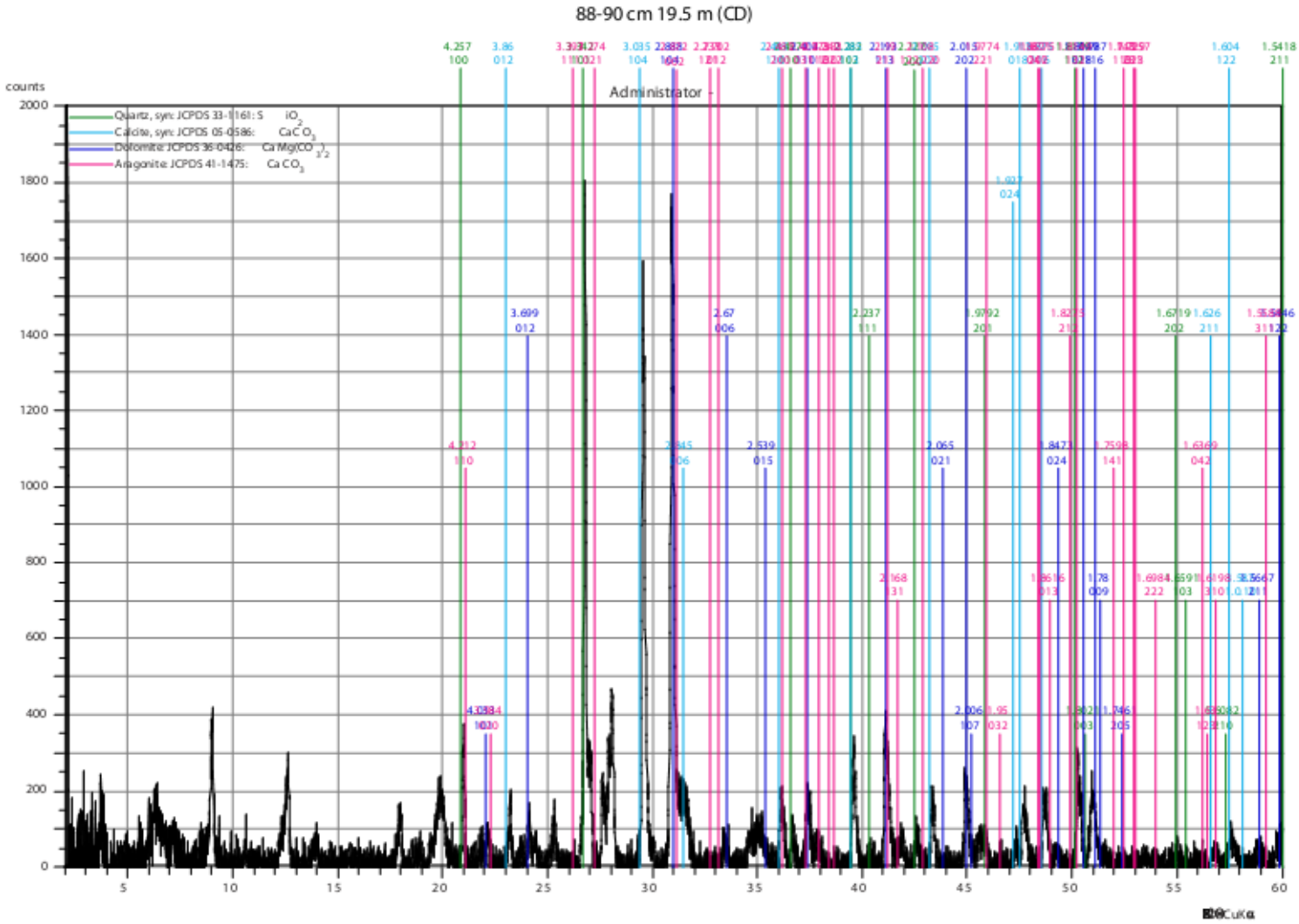

Fig A8: XRD diffractogram of samples from 20.1 m

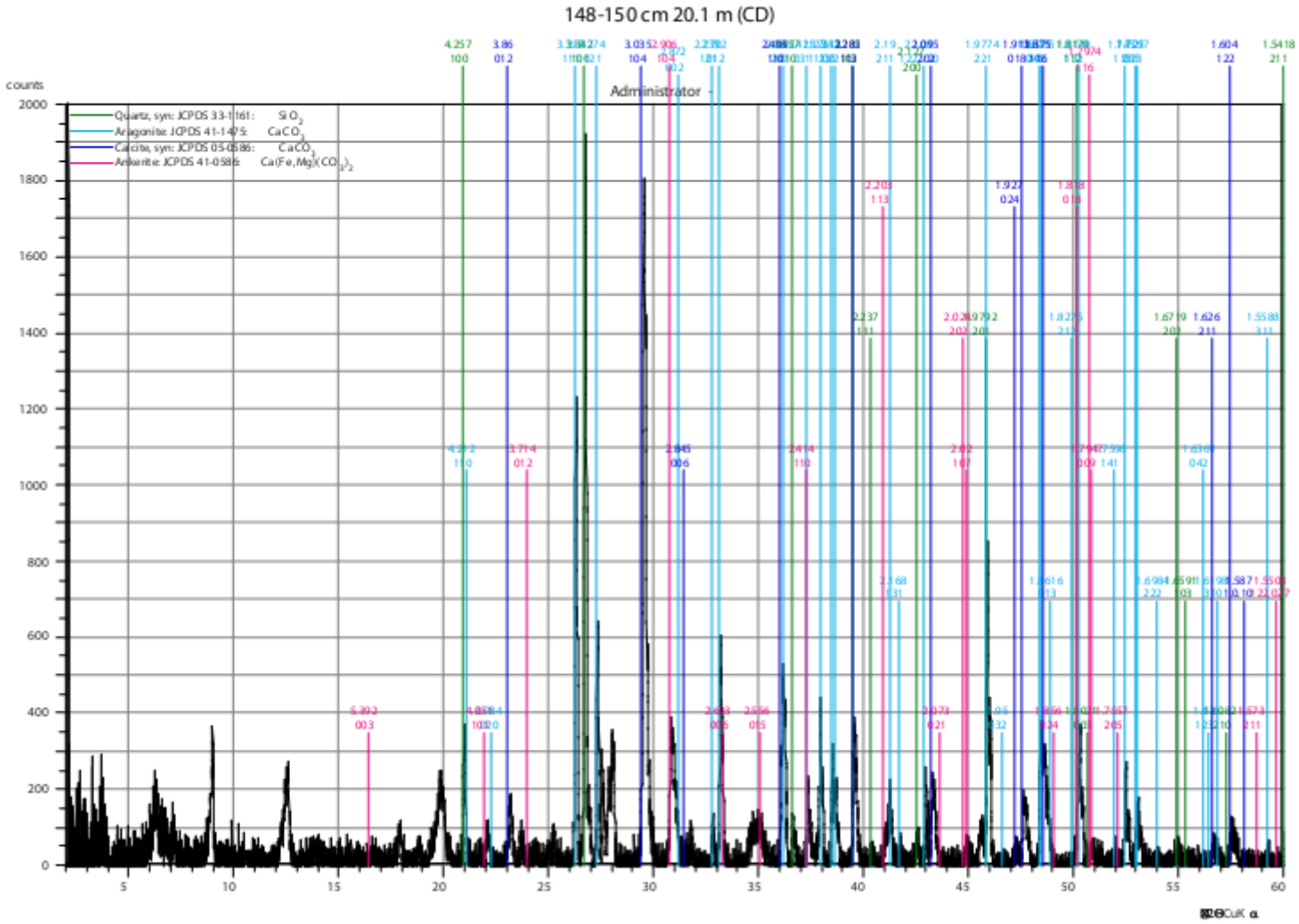

Fig A9: XRD diffractogram of samples from 22.44 m

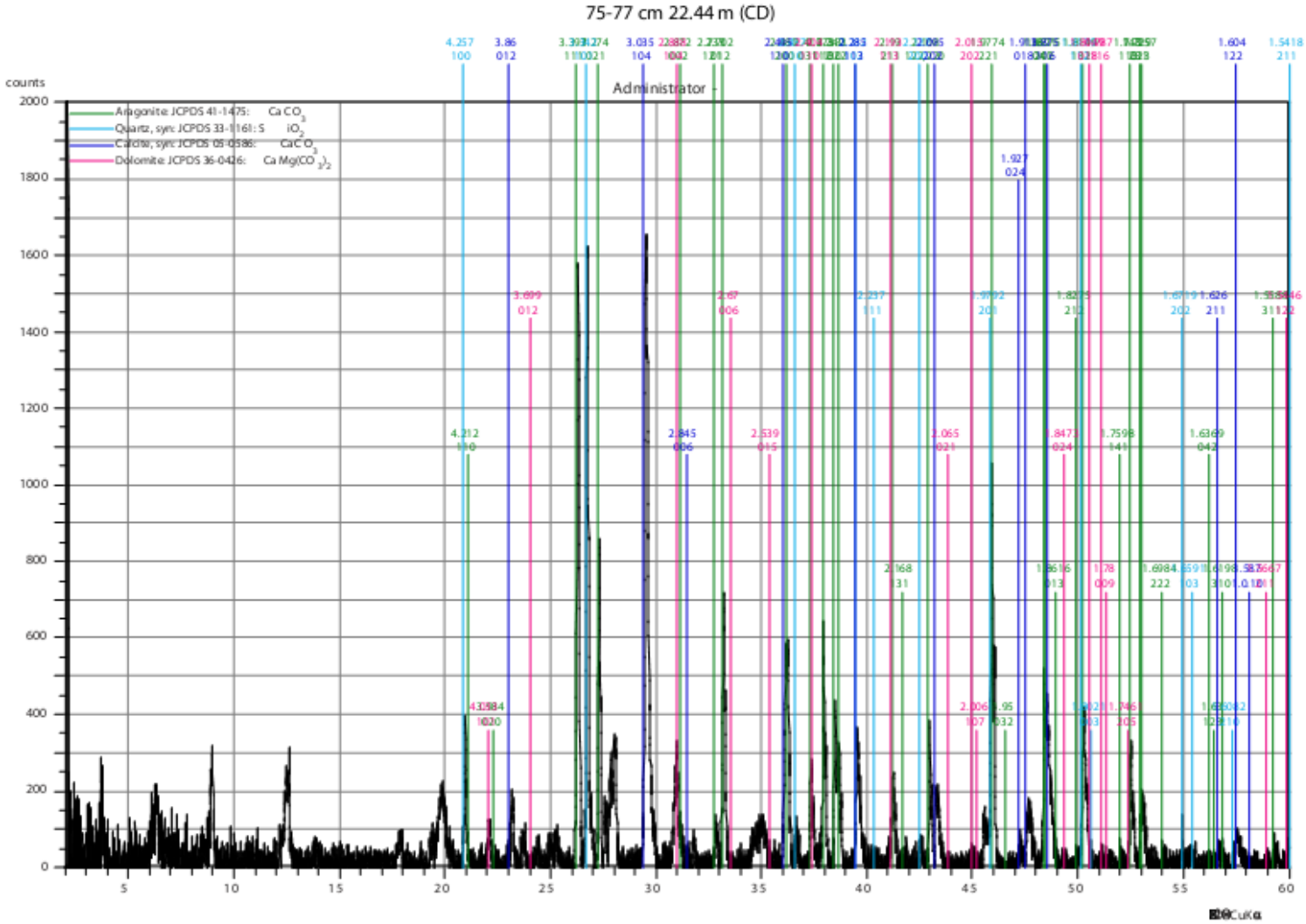

Fig A10: XRD diffractogram of samples from 25.47 m

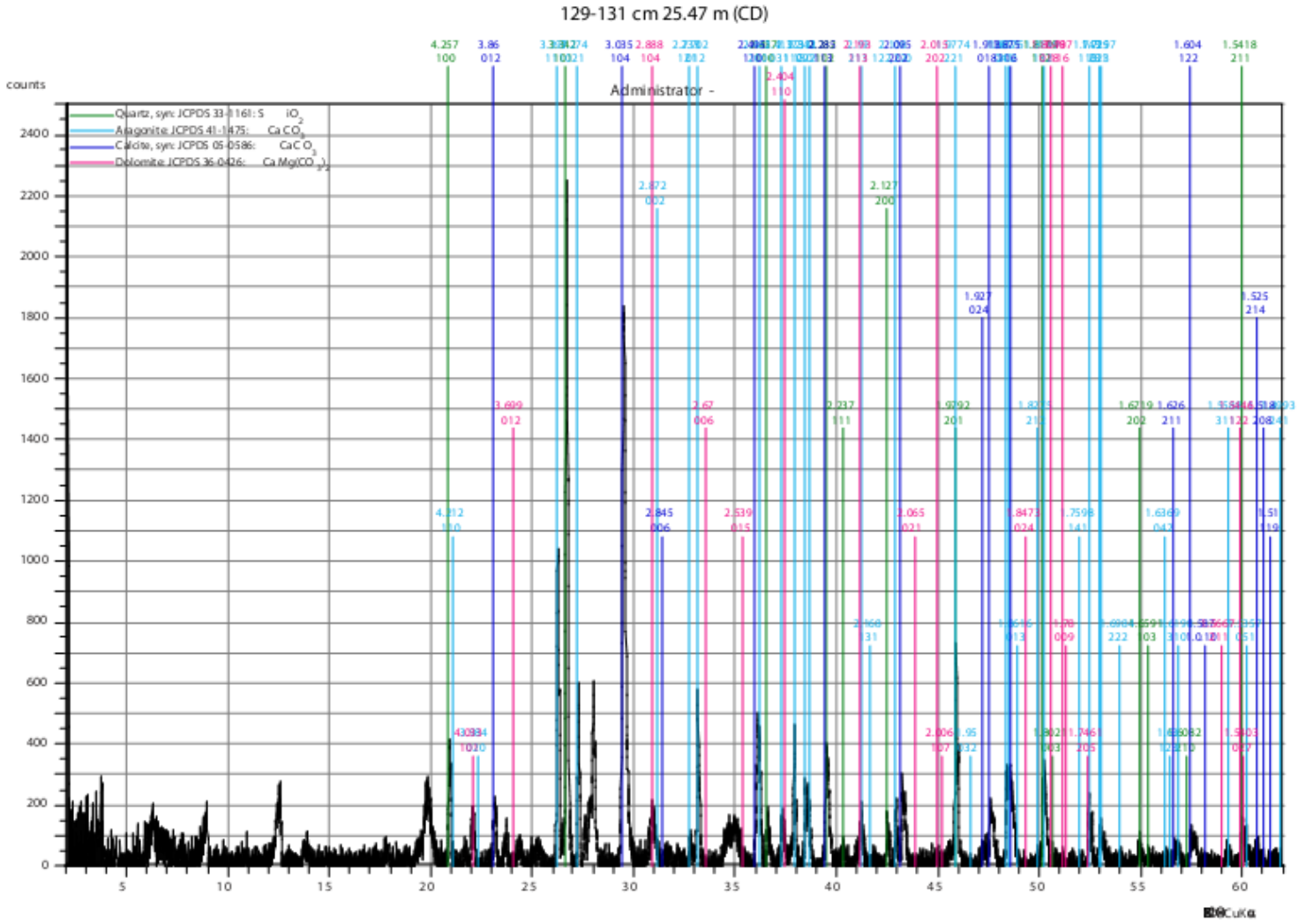

Fig A11: XRD diffractogram of samples from 26.61 m

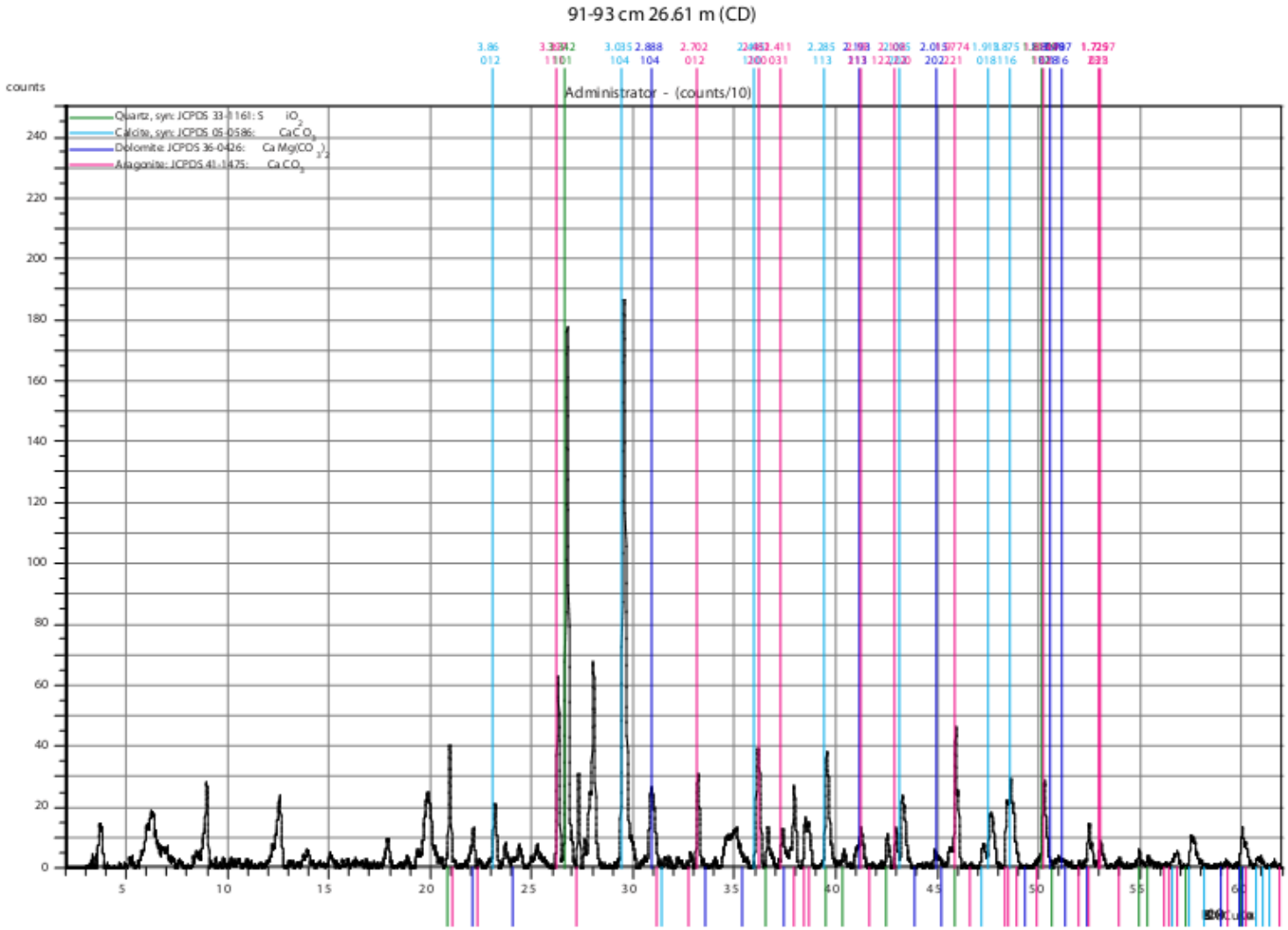

Fig A12: XRD diffractogram of samples from 34.65 m

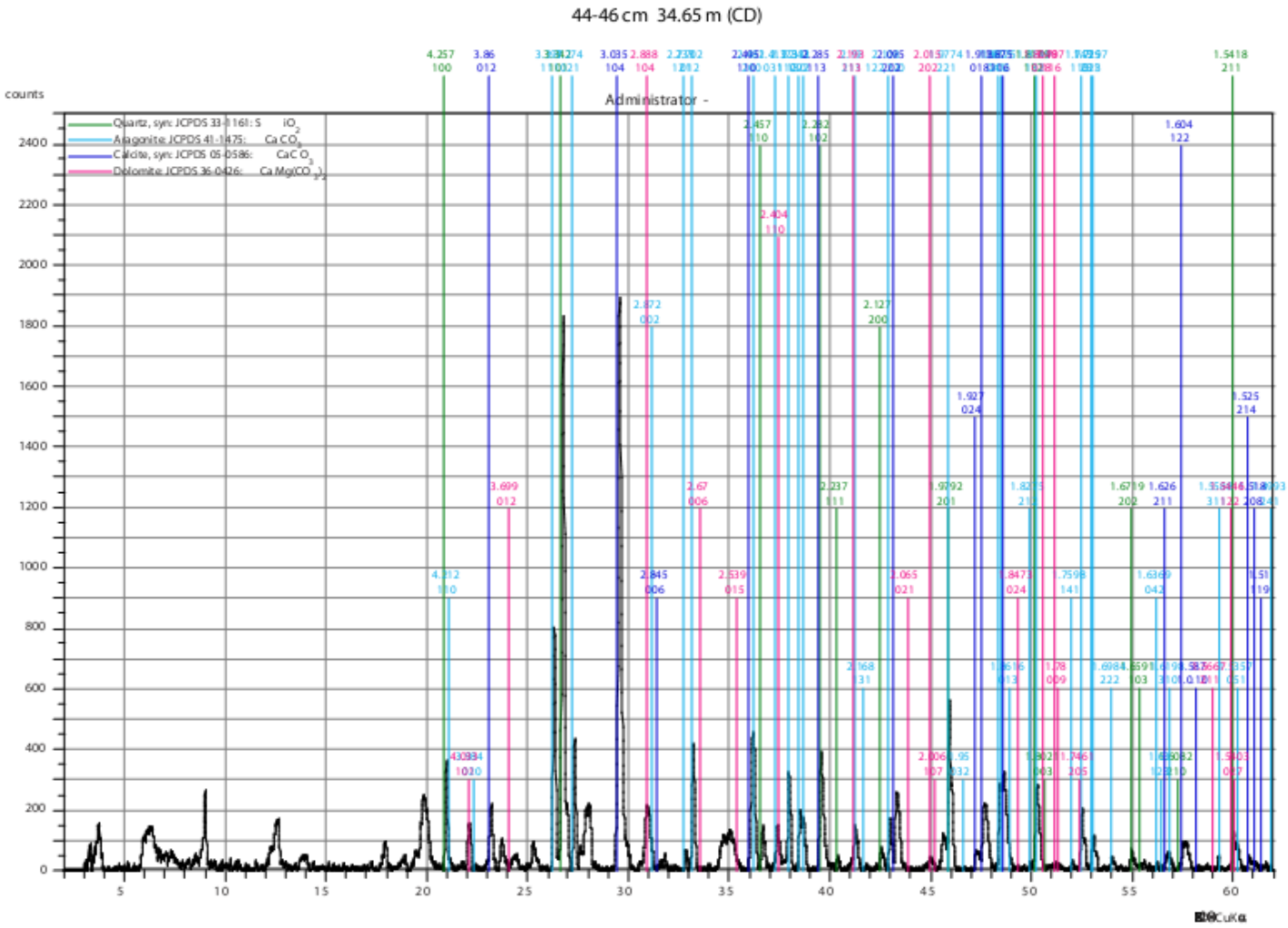

Fig A13: XRD diffractogram of samples from 37.04 m

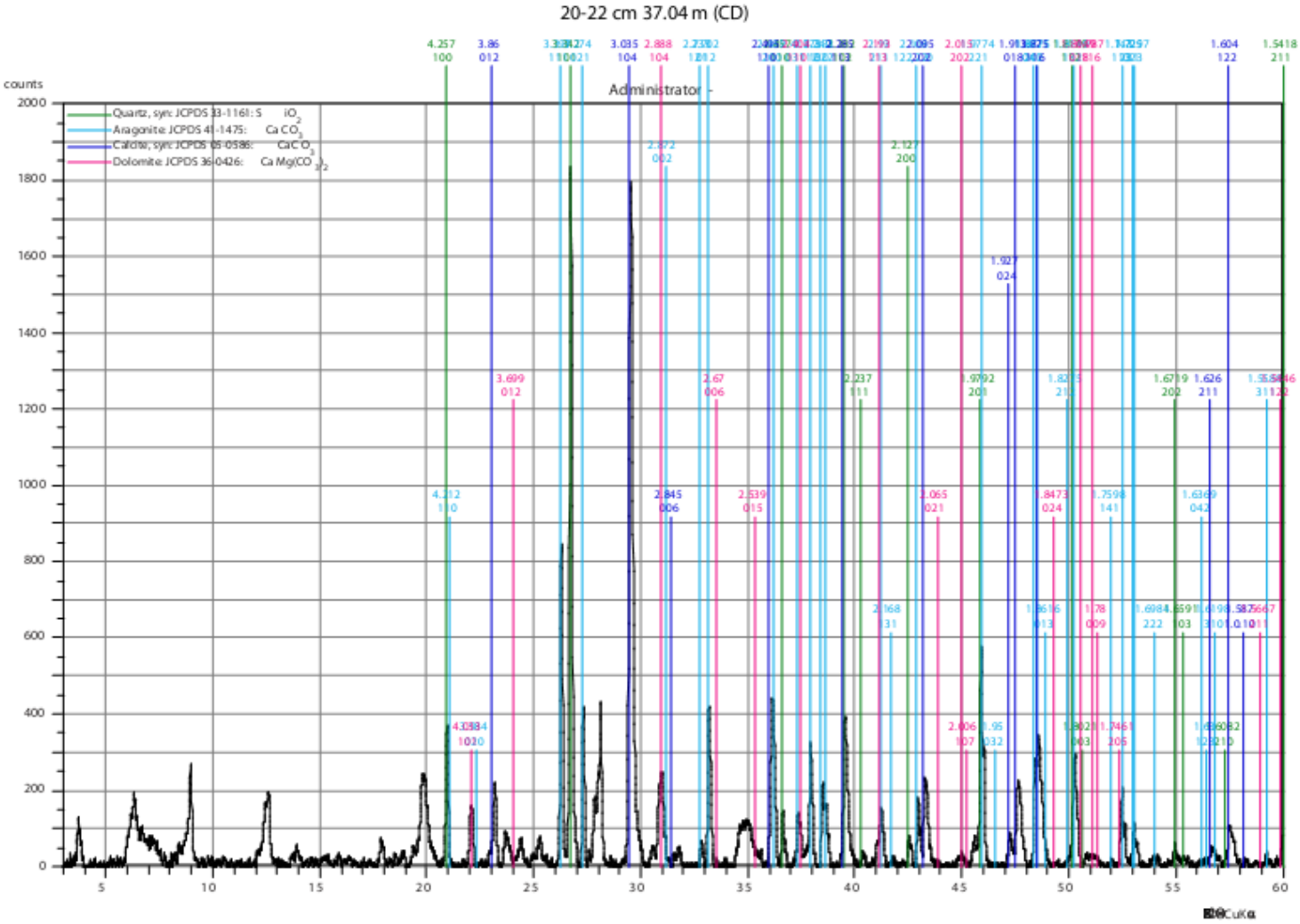

Fig A14: XRD diffractogram of samples from 37.21 m

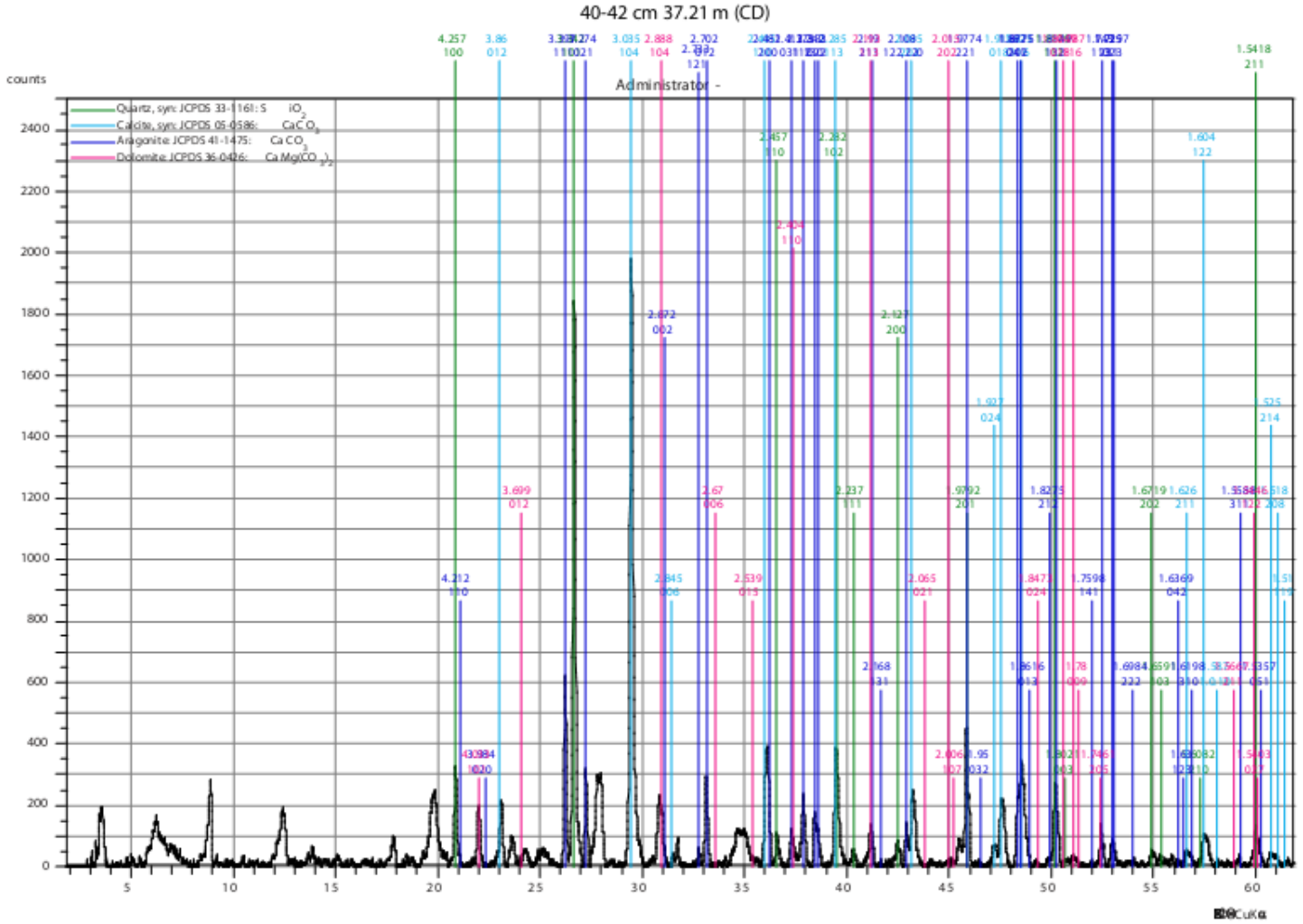

Fig A15: XRD diffractogram of samples from 38.21 m

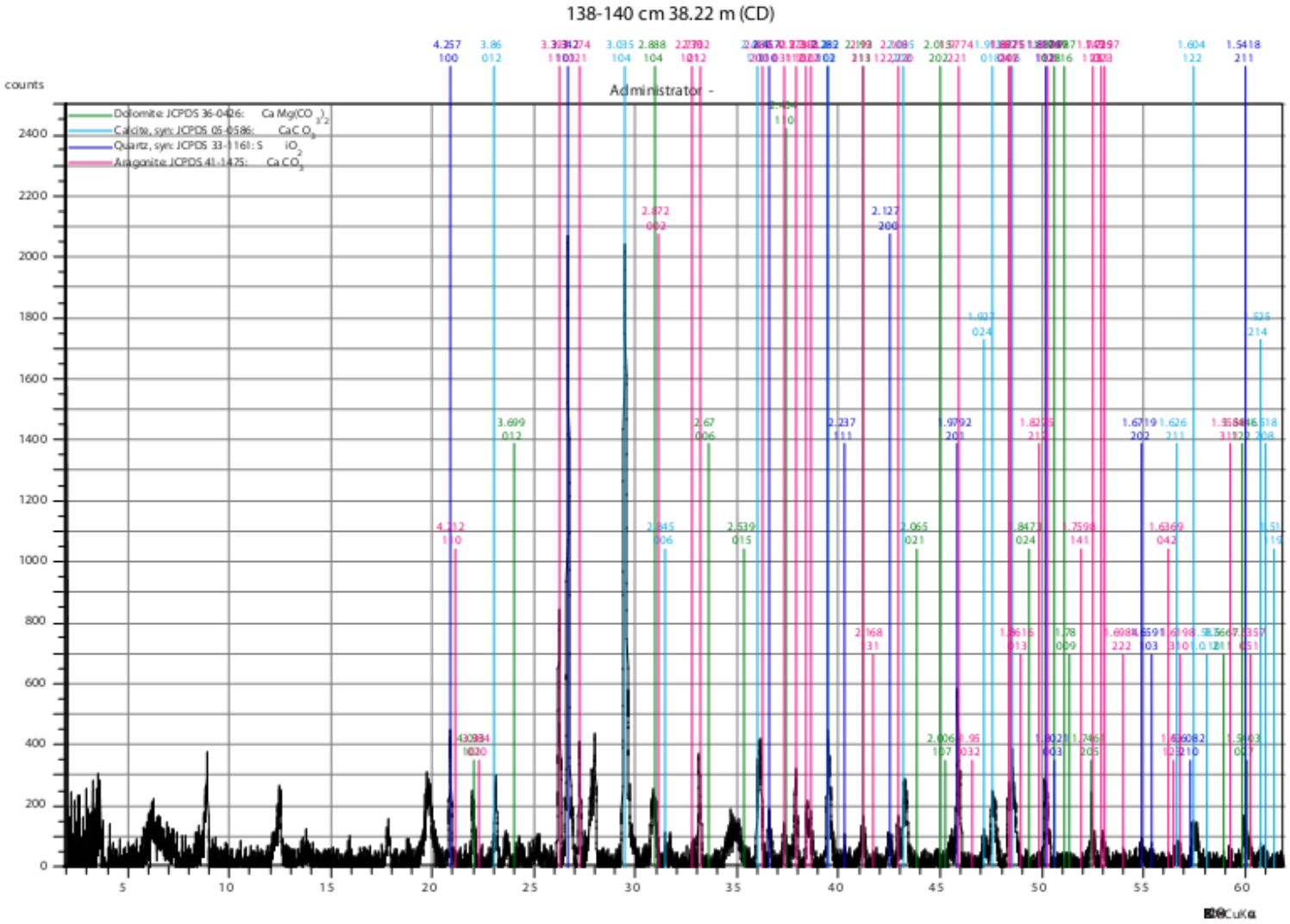

Fig A16: XRD diffractogram of samples from 40.05 m